

NUWC-NPT Technical Report 12,179
30 November 2015

Conceptual Inflatable Fabric Structures for Protective Crew Quarters Systems in Space Vehicles and Space Habitat Structures

Paul V. Cavallaro
NUWC Division Newport

Russell W. Smith
NASA Langley Research Center



**Naval Undersea Warfare Center Division
Newport, Rhode Island**

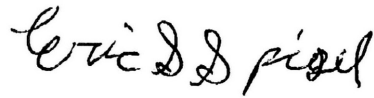
Approved for public release; distribution is unlimited.

PREFACE

This research was sponsored and funded by the National Aeronautics and Space Administration (NASA) Langley Research Center (NASA LaRC), Hampton, VA via an Interagency Agreement. This report was prepared under NUWC Division Newport Assignment Number TD0207, principal investigator Paul V. Cavallaro (Code 7023).

The technical reviewer was Andrew W. Hulton (Code 7023).

Reviewed and Approved: 30 November 2015



Eric S. Spigel
Head, Ranges, Engineering, and Analysis Department



REPORT DOCUMENTATION PAGE

Form Approved
OMB No. 0704-0188

The public reporting burden for this collection of information is estimated to average 1 hour per response, including the time for reviewing instructions, searching existing data sources, gathering and maintaining the data needed, and completing and reviewing the collection of information. Send comments regarding this burden estimate or any other aspect of this collection of information, including suggestions for reducing this burden, to Department of Defense, Washington Headquarters Services, Directorate for Information Operations and Reports (0704-0188), 1215 Jefferson Davis Highway, Suite 1204, Arlington, VA 22202-4302. Respondents should be aware that notwithstanding any other provision of law, no person shall be subject to any penalty for failing to comply with a collection of information if it does not display a currently valid OPM control number.
PLEASE DO NOT RETURN YOUR FORM TO THE ABOVE ADDRESS.

1. REPORT DATE (DD-MM-YY) 30-11-2015		2. REPORT TYPE Technical Report		3. DATES COVERED (From – To)	
4. TITLE AND SUBTITLE Conceptual Inflatable Fabric Structures for Protective Crew Quarters Systems in Space Vehicles and Space Habitat Structures				5a. CONTRACT NUMBER MIPR 8HDAVBW332	
				5b. GRANT NUMBER	
				5c. PROGRAM ELEMENT NUMBER	
6. AUTHOR(S) Paul V. Cavallaro Russell W. Smith				5.d PROJECT NUMBER	
				5e. TASK NUMBER	
				5f. WORK UNIT NUMBER	
7. PERFORMING ORGANIZATION NAME(S) AND ADDRESS(ES) Naval Undersea Warfare Center Division 1176 Howell Street Newport, RI 02841-1708				8. PERFORMING ORGANIZATION REPORT NUMBER TR 12,179	
9. SPONSORING/MONITORING AGENCY NAME(S) AND ADDRESS(ES) NASA Langley Research Center Hampton, VA 23681				10. SPONSORING/MONITOR'S ACRONYM NASA LaRC	
				11. SPONSORING/MONITORING REPORT NUMBER	
12. DISTRIBUTION/AVAILABILITY STATEMENT Approved for public release; distribution is unlimited.					
13. SUPPLEMENTARY NOTES					
14. ABSTRACT This paper describes the development of notional inflatable/deployable secondary structures and their potential for use as inflatable/deployable protective crew quarters systems and inflatable/deployable emergency airlock systems concepts aboard manned spacecraft. These notional structures and their components are described, and their system behaviors are evaluated using an explicit commercial finite element analysis code. Additionally, the effects of inflation pressure and mounting methods on their deployed shapes, wrinkling deformations, volume changes, air masses, limit loads, and textile stresses are characterized and discussed. Of paramount importance to the research described in this research are the lessons learned regarding textile materials and mechanics as related to the development of inflatable/deployable textile structures.					
15. SUBJECT TERMS Inflatable Structures Textiles Protective Textiles Air Beams Woven Fabrics Space Structures Deployable Structures Drop-Stitch Fabrics Finite Element Analysis					
16. SECURITY CLASSIFICATION OF:			17. LIMITATION OF ABSTRACT SAR	18. NUMBER OF PAGES 53	19a. NAME OF RESPONSIBLE PERSON Paul V. Cavallaro
a. REPORT Unclassified	b. ABSTRACT Unclassified	c. THIS PAGE Unclassified			19b. TELEPHONE NUMBER (Include area code) 401-832-5082

TABLE OF CONTENTS

	Page
LIST OF TABLES	iii
LIST OF ABBREVIATIONS, ACRONYMS, AND SYMBOLS	iii
INTRODUCTION	1
Purpose.....	1
Background.....	1
Scope.....	2
SYSTEM CONCEPT DESCRIPTIONS	2
FINITE ELEMENT MODELS.....	6
Ideal Gas Law	6
Cylindrical PCQS FEA Model.....	7
Rectangular PCQS with Inner Membrane Liner FEA Model.....	15
Rectangular PCQS with Embedded Air Beams FEA Model.....	29
SUMMARY AND CONCLUSIONS	43
REFERENCES	44

LIST OF ILLUSTRATIONS

Figure	Page
1 Circular Cylindrical Inflatable Crew Quarters Concept, FEA Model and Section Views: (a) Assembly and (b) Cutaway with Component Details	3
2 Rectangular Inflatable Crew Quarters Concept with Intermediate Air Cushioning Support, FEA Model and Section Views: (a) Assembly and (b) Cutaway with Component Details.....	4
3 Rectangular Inflatable Crew Quarters Concept with Air Beams Embedded in Drop-Stitch Panels, FEA Model and Section Views: (a) Assembly and (b) Cutaway with Component Details	4
4 (a) Actual Drop-Stitch Fabric and (b) Laminated Representation Views.....	5
5 Compression Cycle for a Gas from State 1 to State 2.....	6
6 Displacement (Inches) of the Cylindrical PCQS Concept at 5.0 psig	8
7 Pressurization and Volumetric Responses for the Cylindrical PCQS Up to 5.0 psig.....	8
8 Tension-Running Loads (lbf/in.) for the Cylindrical PCQS Concept at 5.0 psig.....	9
9 Drop-Yarn Tension Force (lbf) of the Cylindrical PCQS Concept at 5.0 psig.....	9
10 Pressurization and Volume Responses for Cylindrical PCQS Concept Up to 10.0 psig...10	10

LIST OF ILLUSTRATIONS (Cont'd)

Figure	Page
11 Displacements (Inches) of the Cylindrical PCQS Concept at 10.0 psig.....	10
12 Tension-Running Loads (lbf/in.) for the Cylindrical PCQS Concept at 10.0 psig.....	11
13 Drop-Yarn Tension Force (lbf) of the Cylindrical PCQS Concept at 10.0 psig.....	11
14 Pressurization and Volume Responses for Cylindrical PCQS Concept Up to 15.0 psig...	12
15 Displacements (Inches) of the Cylindrical PCQS Concept at 15.0 psig.....	12
16 Tension-Running Loads (lbf/in.) for the Cylindrical PCQS at 15.0 psig	13
17 Drop-Yarn Tension Force (lbf) of the Cylindrical PCQS Concept at 15.0 psig.....	13
18 Air Volumes as a Function of Inflation Pressure for the Cylindrical PCQS Concept.....	14
19 Definitions of Ergonomic (a) Planes and Directions and (b) Dimensions.....	15
20 Rectangular PCQS Concept Responses with IML Pressurized to 15.0 psig	16
21 Displacements (Inches) of Rectangular PCQS Concept with IML at 5.0 psig.....	17
22 Tension-Running Loads (lbf/in.) with IML at 5.0 psig	18
23 Drop-Yarn Tension Force (lbf) with IML at 5.0 psig.....	19
24 Rectangular PCQS Concept Responses with IML Pressurized to 10.0 psig	20
25 Displacements (Inches) of Rectangular PCQS Concept with IML at 10.0 psig.....	21
26 Tension-Running Loads (lbf/in.) with Rectangular PCQS Concept IML at 10.0 psig.....	22
27 Drop-Yarn Tension Force (lbf), Rectangular PCQS Concept with IML at 10.0 psig	23
28 Rectangular PCQS Concept Responses with IML Pressurized to 15.0 psig	24
29 Displacements (Inches) of Rectangular PCQS Concept with IML at 15.0 psig.....	25
30 Tension-Running Loads (lbf/in.) with Rectangular PCQS Concept IML at 15.0 psig.....	26
31 Drop-Yarn Tension Force (lbf), Rectangular PCQS Concept, IML at 15.0 psig	27
32 Air Volumes as a Function of Inflation Pressure, Rectangular PCQS Concept, with IML	27
33 Peak Tension-Running Loads (lbf/in.) Versus Pressure, Rectangular PCQS Concept, with IML	28
34 Rectangular PCQS Concept Responses with IML Pressurized to 5.0 psig	30
35 Displacements (Inch), Rectangular PCQS Concept (with Embedded Air Beams) at 5.0 psig.....	31
36 Tension-Running Loads (lbf/in.) with Rectangular PCQS Concept IML at 5.0 psig.....	32
37 Drop-Yarn Tension Force (lbf) of the Rectangular PCQS Concept with IML at 5.0 psig.....	33
38 Rectangular PCQS Concept Responses (with Embedded Air Beams) Up to 10.0 psig	34
39 Displacements (Inch), Rectangular PCQS Concept (with Embedded Air Beams) at 10.0 psig.....	35
40 Stresses (psi) of Rectangular PCQS Concept (with Embedded Air Beams) at 10.0 psig.....	36
41 Drop-Yarn Tension Force (lbf) of PCQS Concept (with Embedded Air Beams) at 10.0 psig.....	37
42 Responses for Rectangular PCQS Concept (with Embedded Air Beams) Up to 15.0 psig.....	38
43 Displacements (Inch), Rectangular PCQS Concept (with Embedded Air Beams) at 15.0 psig.....	39

LIST OF ILLUSTRATIONS (Cont'd)

Figure		Page
44	Stresses (psi) of Rectangular PCQS Concept (with Embedded Air Beams) at 10.0 psig.....	40
45	Drop-Yarn Tension Force (lbf) of PCQS Concept (with Embedded Air Beams) at 15.0 psig.....	41
46	Air Volumes, Rectangular PCQS Concept (with Embedded Air Beams) Versus Pressure.....	41
47	Peak Tension Running Loads (lbf/in.), Rectangular PCQS (with Embedded Air Beams)	42

LIST OF TABLES

Table		Page
1	Minimum Design and Test Factors for Structural Soft Goods	2
2	Component Air Volumes of the Rectangular PCQS Concept with Inner Membrane Liner	27
3	Skin Tension Force per Unit Length Results of the Rectangular PCQS Concept with IML	28
4	Component Air Volumes of the Rectangular PCQS Concept with Embedded Air Beams	41
5	Skin Tension Force per Unit Length Results of the Rectangular PCQS Concept with Embedded Air Beams	42

LIST OF ABBREVIATIONS, ACRONYMS, AND SYMBOLS

3-D	Three-dimensional
A	Height
B	Shoulder depth
B/G	Ratio of shoulder width to depth
C	Constant
D_{cylinder}	Diameter of the cylindrical concept
EALS	Emergency airlock system
$E_{\text{dissipative}}$	Dissipative energy
E_{internal}	Internal energy
E_{kinetic}	Kinetic energy
E_{strain}	Strain energy
F	Force

LIST OF ABBREVIATIONS, ACRONYMS, AND SYMBOLS (Cont'd)

F	Total reach span
FEA	Finite element analysis
FSI	Fluid/structure interactions
G	Shoulder depth
GCR	Galactic cosmic rays or radiation
HPF	High-performance fibers
IML	Inner membrane liner
K	Degree Kelvin
LaRC	Langley Research Center
m	Mass
Max	Maximum
NASA	National Aeronautics and Space Administration
NASA-STD	NASA Technical Standard
n	Ratio of specific heats
P	Absolute pressure
PBS	Physics-based simulations
PCQS	Protective crew quarters system
R	Universal gas constant
SPE	Solar particle event
T	Absolute temperature
V	Volume
δ	Displacement (deflection at point of loading)
Δ	Change from inflation step to applied loading step

CONCEPTUAL INFLATABLE FABRIC STRUCTURES FOR PROTECTIVE CREW QUARTERS SYSTEMS IN SPACE VEHICLES AND SPACE HABITAT STRUCTURES

INTRODUCTION

PURPOSE

The confluence of several inflatable structures technologies and finite element modeling capabilities has made air-inflated fabric structures viable options for many industries. Advancements such as high-performance fibers and fabrics, three-dimensional (3-D) continuous-woven architectures, protective and flexible coatings, multi-axial material-level testing, and predictive-performance-analysis methods that enable virtual design processes¹⁻¹³ are key technological enablers for achieving new, unprecedented applications for inflatable and deployable structures that can be designed as alternatives to traditional rigid structures.

Inflatable structures provide unique operational advantages and significant weight savings; moreover, they are capable of deployed-to-stowed volume ratios that are particularly attractive for aerospace-related applications. This report describes the development of notional inflatable/deployable secondary structures and their potential for use as inflatable/deployable protective crew quarters systems (PCQS) and inflatable/deployable emergency airlock systems (EALS) concepts aboard manned spacecraft.

This report describes these notional inflatable structures and their components and evaluates their system behaviors using the Abaqus/Explicit finite element analysis (FEA) code.¹⁴ Additionally, the effects of inflation pressure and mounting methods on their deployed shapes, wrinkling deformations, volume changes, air masses, limit loads, and textile stresses are characterized and discussed. Of paramount importance to the research documented in this report are the lessons learned regarding textile materials and mechanics as related to the development of inflatable/deployable textile structures, now referred to as “fabric structures.”

BACKGROUND

Space vehicles and systems are subject to critical restrictions that both affect and define their mission roles, safety requirements, and payload capacities. Always present, however, is the unwavering focus on minimizing cost, weight, and volume of onboard hardware while maximizing architectural efficiencies and mission effectiveness levels.

Inflatable/deployable textile structures provide significant benefits as alternatives to traditional rigid structures; their increased use in military and commercial applications is

attributed to the combined use of high-performance fibers (HPF) and continuous weaving methods. Recent advances in fiber materials, coatings, and technical textile processing methods have enabled the next-generation of “soft goods” to achieve significant load-carrying capacities while preserving their inherent use-on-demand, minimal weight, and efficient stowed-volume characteristics. Physics-based simulations (PBS) have recently been developed as virtual design tools. These design tools, coupled with validation testing, provide a reliable and invaluable approach for achieving superior design efficiencies and optimized solutions.

Strength requirements for inflatable structures (excluding deployable decelerator systems, such as parachutes, parafoils, airbags, inflatable heat shields, and similar systems) are governed by strength specifications for soft goods as described in NASA-STD-5001B.¹⁵ The load and proof test factors are listed in table 1. Note that habitable modules are not considered pressure vessels. These factors will become particularly useful for developing and testing physical prototypes of the various PCQS concepts that are evaluated in the present study using PBS.

Table 1. Minimum Design and Test Factors for Structural Soft Goods

Hardware Criticality Classification	Ultimate Design Factor	Prototype Test Factor	Proof Test Factor
Loss of Life or Vehicle	4.0	4.0	1.2
All Others	2.0	2.0	1.2

SCOPE

This research had two primary goals: (1) to demonstrate the applicability of today’s air-inflated fabric structures technologies for developing notional concepts of inflatable/deployable PCQSs and inflatable/deployable EALSs having minimal weight, minimal stowed volume, and fail-safe wrinkling mechanisms using PBS methods and (2) to leverage previous experimental and computational mechanics research involving air-inflated woven fabric beams and drop-stitch fabric panels.

SYSTEM CONCEPT DESCRIPTIONS

Secondary structures with relevance to human spacecraft systems are those structures internal to the life-support boundaries of the spacecraft. The crew quarters are configured within the crew module of the spacecraft; they are the zones in which crew members generally do not require wearing additional devices or protections to maintain and preserve life. One notable exception occurs when spacecraft are subject to extreme radiation levels caused by either solar particle events (SPEs) or galactic cosmic rays (GCRs). SPEs emit high amounts of solar energy through the release of protons—a form of radiation. SPEs can compromise the physiological and immune systems of astronauts; therefore, additional protection is required to shield the astronauts

against such radiation when they are residing within the crew quarters. It is necessary, therefore, to provide astronauts with a temporary protective enclosure that is rapidly deployable and lightweight, provides simple ingress/egress modes of operation, and, if possible, can be assembled from dual-purpose, readily available portable and stowable items. The issues of GCR protection are much more complex than those associated with SPEs; water shielding, however, will also help with such radiation conditions.

Several inflatable/deployable PCQS concepts were developed as individualized, hand-assembled protective enclosures as shown in figures 1–3. These concepts are generally simple to operate, with each consisting of multiple, fillable volumes configured with drop-stitch fabric panels that, when assembled using retention straps and Velcro fastening strips, fully encompass the astronaut. Woven-fabric air beams are included in the rectangular concepts to serve as deployment enabler elements. Once inflated with air, the air beams generate a skeletal frame to which the drop-stitch panels are hand attached and secured using the retention straps. For the protection of astronauts against SPEs, the volumes are filled with water, resulting in a 4.0-inch layer along the perimeters of each enclosure. When the enclosures are placed side by side, the effective transverse thickness becomes approximately 8 inches, which equates to the optimal shielding ratio of 20 g/cm^2 specified by Slaba et al.¹⁶ Given that the density of water = 1 g/cm^3 , this configuration yields a thickness of 20 cm (or 7.874 inches). Increasing the shielding ratio beyond this value provides no substantial increase in shielding levels. The spacecraft material, along with its associated infrastructure and logistics, would help ameliorate the radiation conditions in the other directions associated with the back-to-back crew quarters, and it could possibly be arranged strategically for impending SPEs (also known as solar flares). The water-filled panels are constructed from drop-stitch fabrics, a type of 3-D woven pre-form, also known as spacer fabrics, and include positive-locking fill/drain ports. The water-filled drop-stitch panels can serve the redundant role as water storage bags currently used in spacecraft missions.

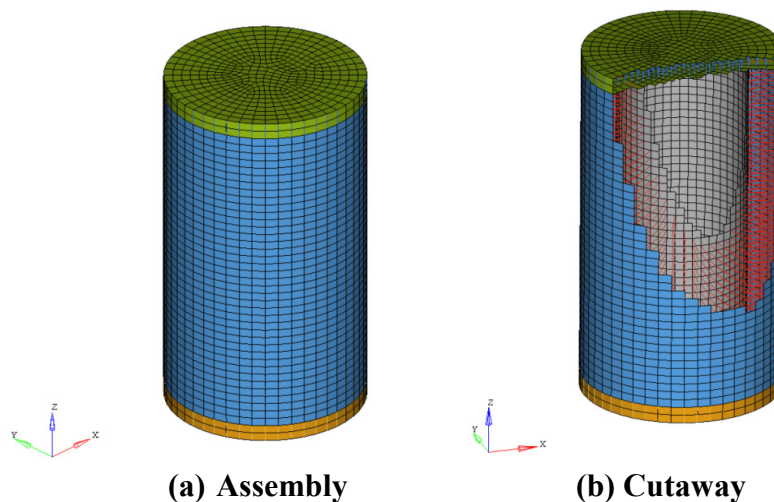


Figure 1. Circular Cylindrical Inflatable Crew Quarters Concept, FEA Model and Section Views: (a) Assembly and (b) Cutaway with Component Details

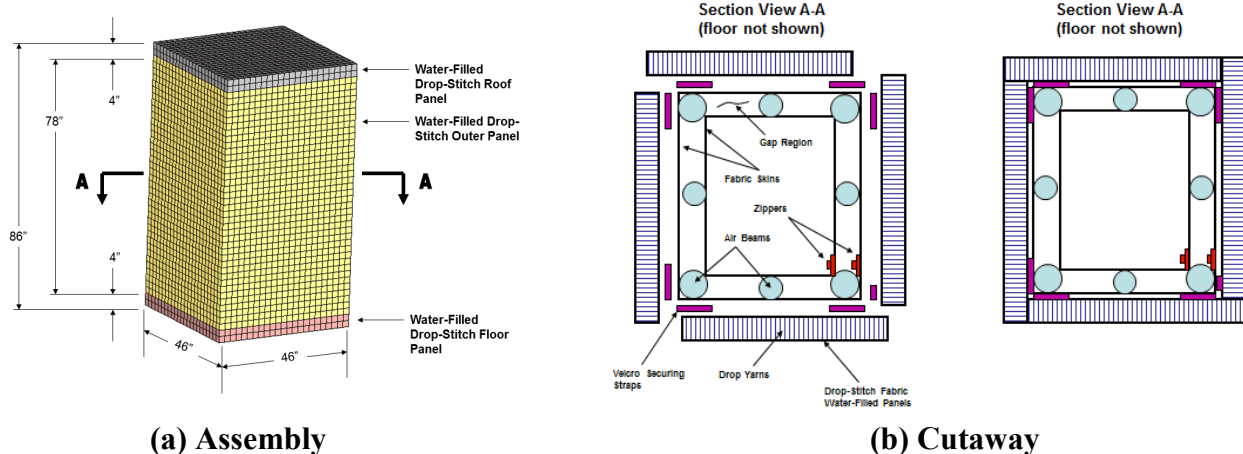


Figure 2. Rectangular Inflatable Crew Quarters Concept with Intermediate Air Cushioning Support, FEA Model and Section Views: (a) Assembly and (b) Cutaway with Component Details

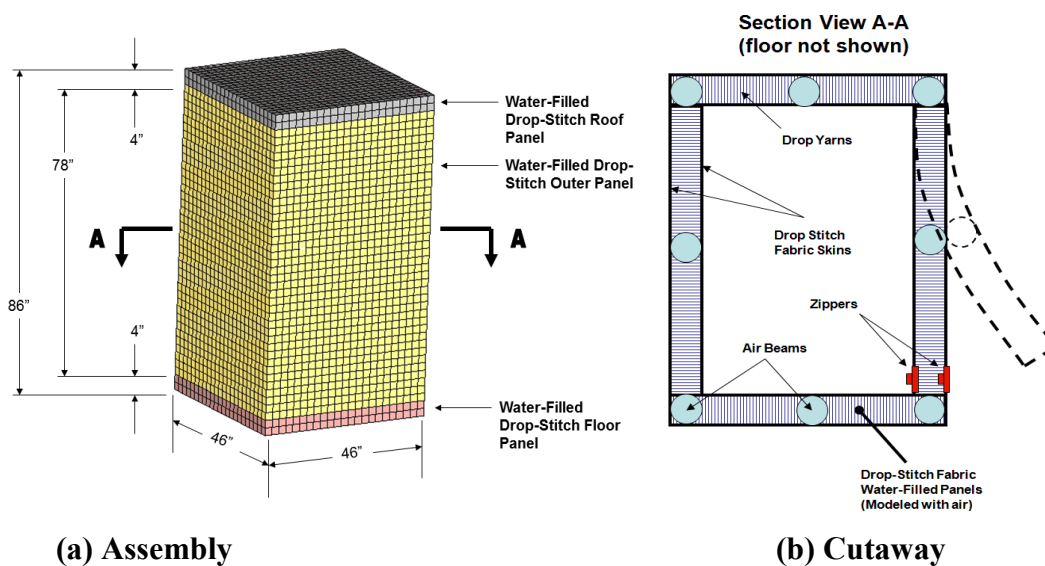


Figure 3. Rectangular Inflatable Crew Quarters Concept with Air Beams Embedded in Drop-Stitch Panels, FEA Model and Section Views: (a) Assembly and (b) Cutaway with Component Details

The construction details of a typical drop-stitch woven fabric are illustrated in figure 4. A drop-stitch fabric is a type of 3-D, integrally and continuously woven textile product that resembles sandwich panels having two woven face sheets separated by a distance equal to the length of the drop yarns. The face sheets consist of two warp yarn families and one weft yarn family. One of the two warp yarn face sheets is known as a drop-yarn type; the drop yarns are periodically “dropped” from one deck layer to the other and back again. For air-inflated structural applications, rubber-like coatings are laminated over the surfaces of the drop-stitch skins. The edges of the drop-stitched panels are then closed and sealed, and the coatings behave as a bladder to contain the volume of pressurized air (or other gas or fluid media).

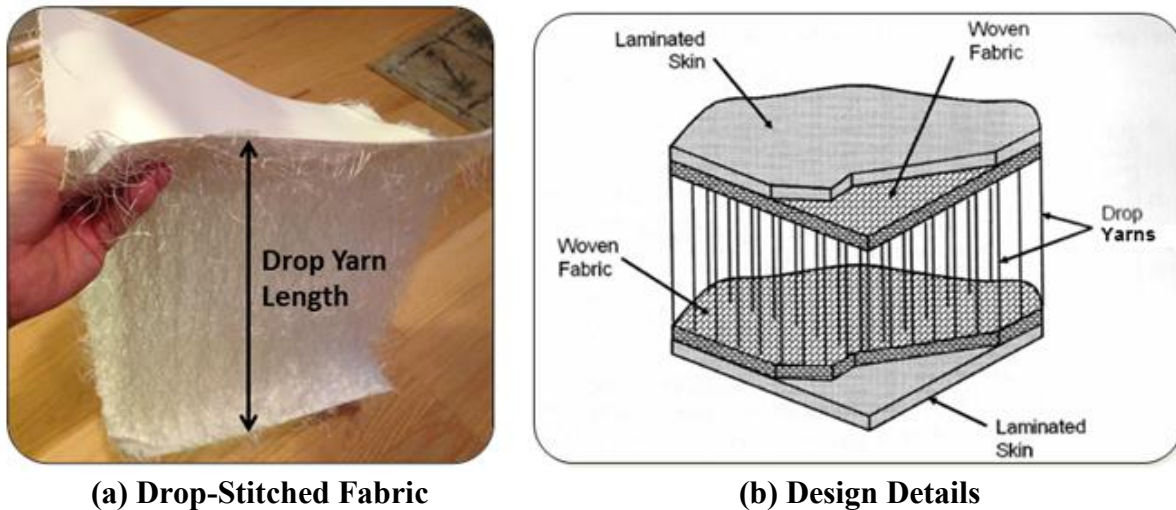


Figure 4. (a) Actual Drop-Stitch Fabric and (b) Laminated Representation Views

A key advantage to using the drop-stitched pre-form is its ability to develop a flat-like panel when it is inflated or filled with a fluid. Flatness and parallelism of the face sheets are achieved by increasing the number of drop yarns per unit area and by increasing the extensional stiffness of the drop yarns. The construction used during this research consisted of drop yarns that were 32 yarns/in.², with the potential to be tailored up to 64 yarns/in.², thus providing an inherent ability to stiffen the structure in strategic locations.

The advantages of an all-fabric structural system include efficient packability for achieving minimal stowage volume and the uniquely inherent structural fail-safe mechanism of wrinkling rather than fracture when the structure is overloaded. During an overload event, the drop-stitch fabric structure simply wrinkles; upon restoration to the proper operating loads, the structure returns to its design configuration without damage.

FINITE ELEMENT MODELS

IDEAL GAS LAW

Finite element modeling of each PCQS concept was performed using Abaqus/Explicit. Model details such as drop-stitch material properties, skin thicknesses, drop-yarn cross-sectional areas and areal densities (number of drop yarns per unit area), and methods of inflation were leveraged when possible from a prior study.¹³ Displacement boundary conditions were implemented based on expected operational restraints. The woven air beams and drop-stitch skins were modeled as isotropic membranes; the drop yarns were modeled as tension-only string elements. Linear elastic properties were assigned to each material. The ideal gas law shown in equation (1) governed the pressure-volume relationship for each air volume and is given by

$$PV = mRT, \quad (1)$$

where P is the absolute pressure, V is the volume of air, m is the mass of air, R is the ideal gas constant, and T is the absolute temperature (°K). Additionally, for a polytropic thermodynamic process,¹⁷ the pressure-volume relationship for the compression cycle of a gas, shown in figure 5, is described using equation (2),

$$PV^n = C, \quad (2)$$

where $C = \text{constant}$, and $n = \text{the ratio of specific heats}$ ($n = 1.4$ for air).

Two states of a polytropic compression (or expansion) process therefore can be described by equation (3),

$$P_1V_1^n = P_2V_2^n, \quad (3)$$

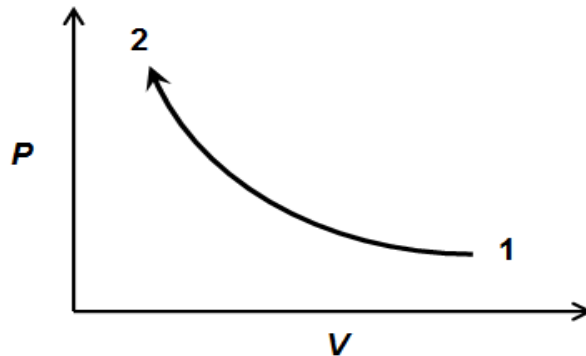


Figure 5. Compression Cycle for a Gas from State 1 to State 2

Fluid-structure interactions (FSIs) occur when the enclosed air (fluid) experiences pressure and volume changes resulting from panel deformations due to applied mechanical and thermal loads. Additionally, tensile strains can develop in the membrane material that will, for a closed system, contribute to volume increases. This type of fluid-structure coupling, which is unique to inflated structures, is a source of nonlinear behavior. This coupling increases the complexity of the governing mechanics. When FSIs are significant, air compressibility must be included in the energy balance because, in addition to the strain energy developed in the membrane materials, the thermodynamic work done on the air, known as PV-work, must be accounted for.

The idealized form of the energy balance for an air-inflated fabric structure is given by equation (4),

$$\int Fd\delta = \Delta E_{\text{internal}} = \Delta E_{\text{strain}} + \Delta E_{\text{kinetic}} + \Delta E_{\text{dissipative}} + \Delta \int PdV + \Delta \int VdP, \quad (4)$$

where F is an externally applied force, δ is the deflection at point of loading, E_{internal} is the internal energy of the system, E_{strain} is the sum of the elastic (recoverable) and plastic (irrecoverable) strain energies, E_{kinetic} is the kinetic energy of the system mass, and $E_{\text{dissipative}}$ is the dissipated energy through damping and viscous effects. The δ symbol is used to denote differences between inflated and externally loaded states; the Δ symbol is used to denote change from inflation step to applied loading step.

The models accounted for the FSIs resulting from the combined material deformations and air compressibilities within each air volume. The governing energy balance included the strain energies developed within each material and the PV-work done on the air volumes as previously denoted by equation (4).

CYLINDRICAL PCQS FEA MODEL

The initial PCQS concept shown in figure 1 was a circular, cylindrical construct assembly with flat end panels. The cylindrical concept was expected to provide the least weight and largest deployed-to-stowed volume ratio. The cylindrical concept, however, had significant structural and ergonomic drawbacks. The major structural drawback was its inability to properly develop tension along the circumferential direction of the inner drop-stitch skin; the drop-stitch fabric panels were inflated with air and were not filled with water. During inflation of the cylindrically shaped drop-stitch component, the air pressure increased the radius of curvature (and circumference) of the outer skin, thereby enabling it to readily achieve a necessary biaxial state of tension. The air pressure, however, forced the inner skin to decrease its radius of curvature (and circumference), which caused the inner skin to go slack and consequently prevented it from initially achieving a state of biaxial tension. To achieve static equilibrium with increasing inflation pressure, the inner skin had to grossly deflect radially inward toward the center of the cylinder, which resulted in highly nonuniform wall thicknesses (that is, ballooning).

The ergonomic drawback was the loss of compartment volume for the crew member, or astronaut. The excessive deflections of the inner skin highly encroached upon the available volume in the cylindrical PCQS concept. This encroachment is shown in the deflection contour plots in figure 6 and in the air pressure- and air volume-time history plots in figure 7. The time history plots also indicate that the internal volume of the cylindrical drop-stitch layer required significantly greater air mass to achieve static equilibrium at a prescribed inflation pressure in comparison to the mass of air required for the following rectangular PCQS concepts at the same pressure.

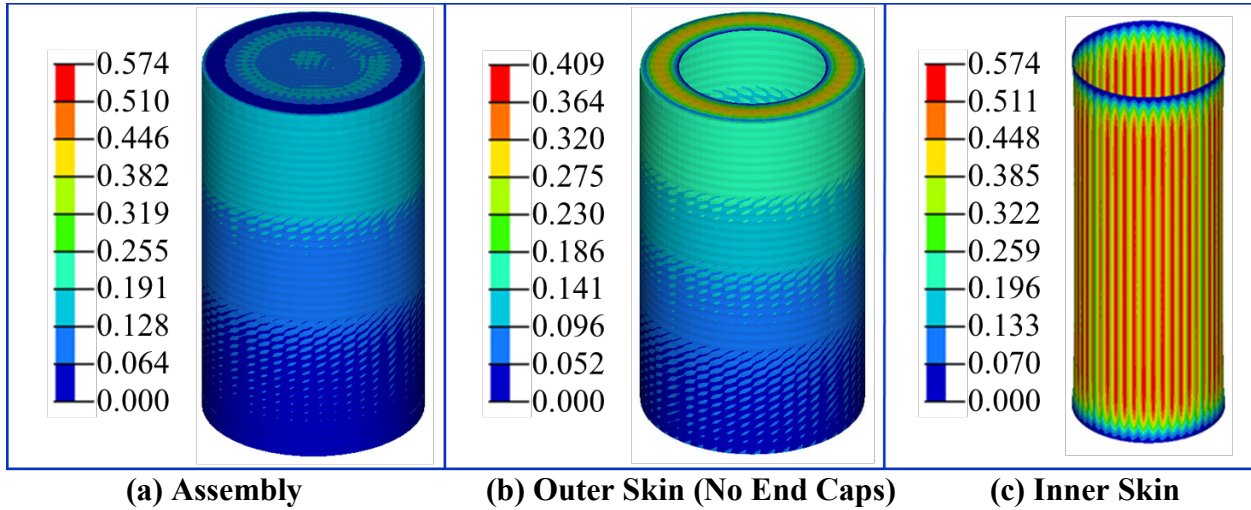


Figure 6. Displacement (Inches) of the Cylindrical PCQS Concept at 5.0 psig

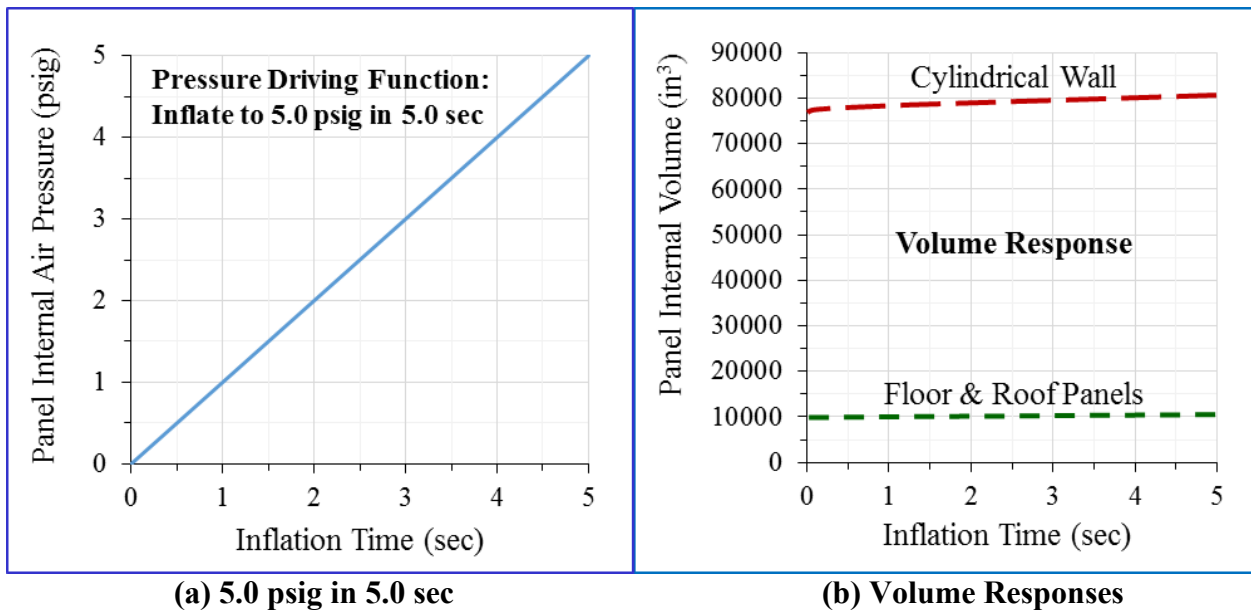


Figure 7. Pressurization and Volumetric Responses for the Cylindrical PCQS Up to 5.0 psig

Figures 8 and 9 are contour plots of the skin tensions per unit length (running loads) and the drop-yarn tension forces, respectively, for the 5.0-psig inflation pressure. Figures 10–17 show the results of the cylindrical PCQS concept at inflation pressures of 10.0 and 15.0 psig.

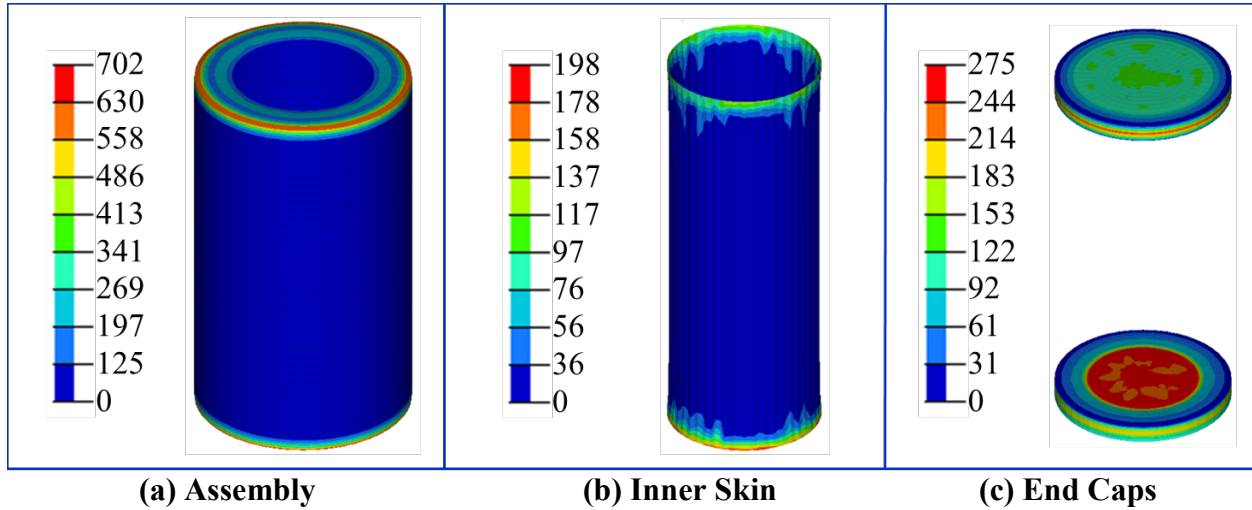


Figure 8. Tension-Running Loads (lbf/in.) for the Cylindrical PCQS Concept at 5.0 psig

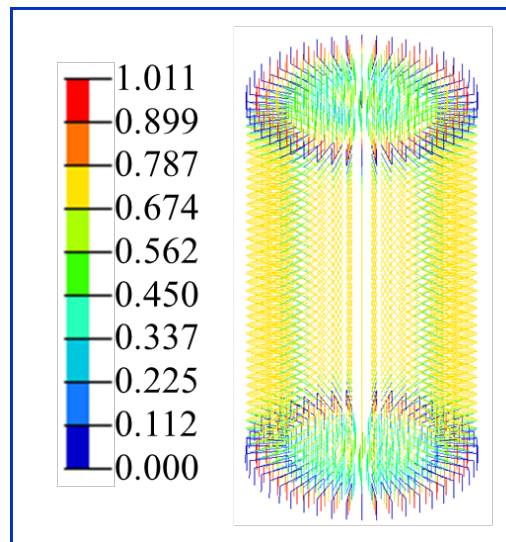
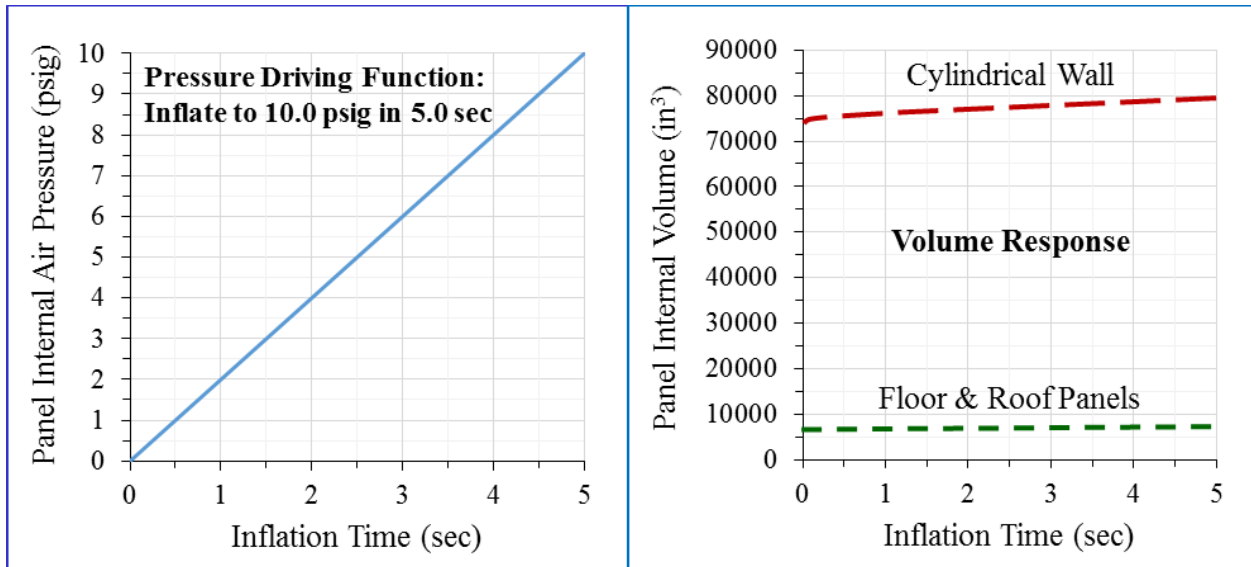


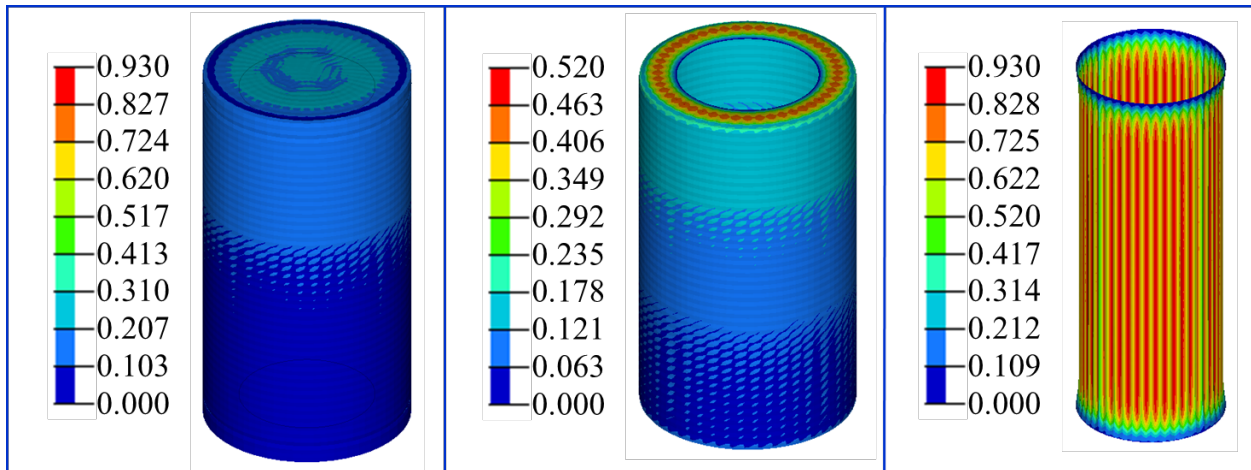
Figure 9. Drop-Yarn Tension Force (lbf) of the Cylindrical PCQS Concept at 5.0 psig



(a) 10.0 psig in 5.0 sec

(b) Volume Responses

Figure 10. Pressurization and Volume Responses for Cylindrical PCQS Concept Up to 10.0 psig



(a) Assembly

(b) Outer Skin (No End Caps)

(c) Inner Skin

Figure 11. Displacements (Inches) of the Cylindrical PCQS Concept at 10.0 psig

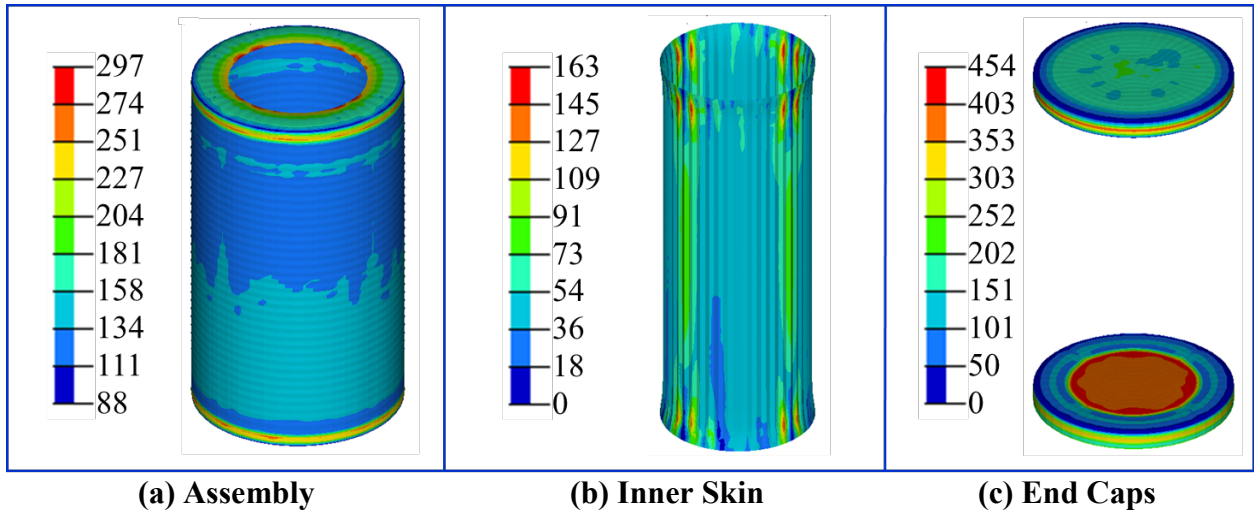


Figure 12. Tension-Running Loads (lbf/in.) for the Cylindrical PCQS Concept at 10.0 psig

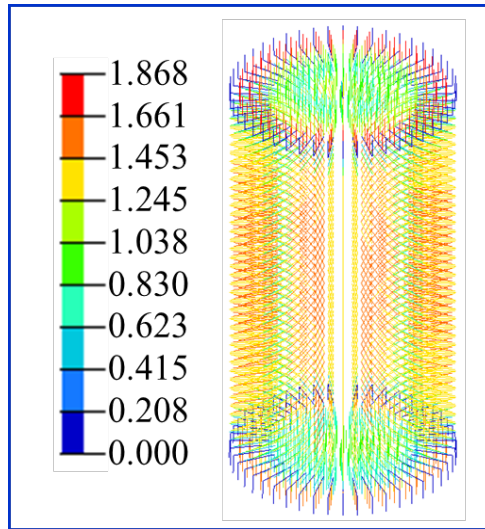
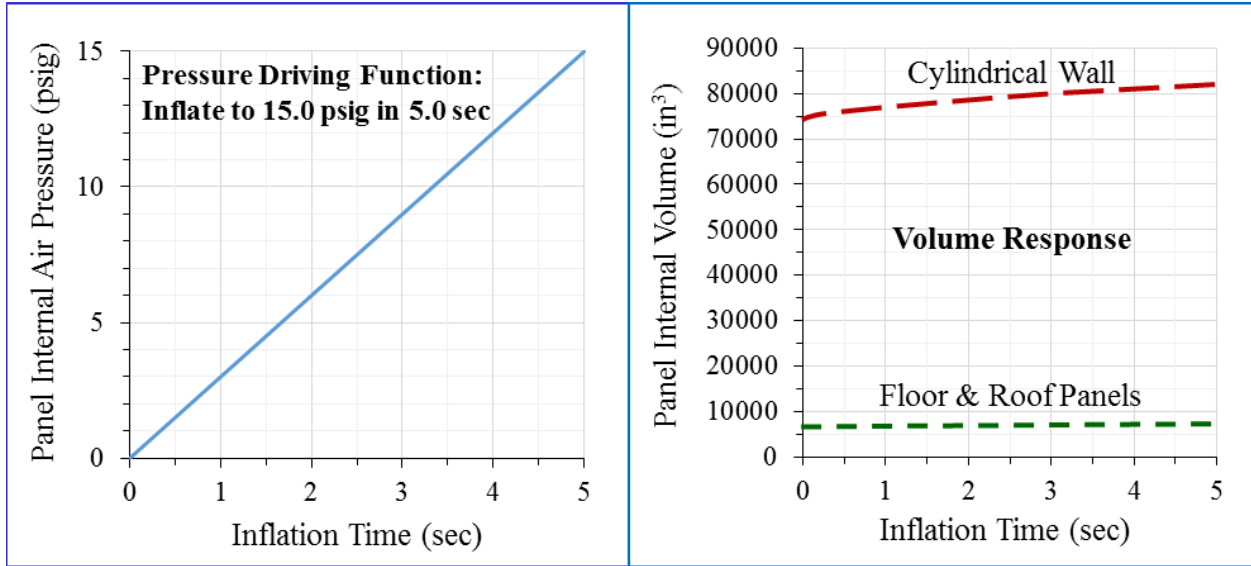


Figure 13. Drop-Yarn Tension Force (lbf) of the Cylindrical PCQS Concept at 10.0 psig



(a) 15.0 psig in 5.0 sec **(b) Volume Responses**

Figure 14. Pressurization and Volume Responses for Cylindrical PCQS Concept Up to 15.0 psig

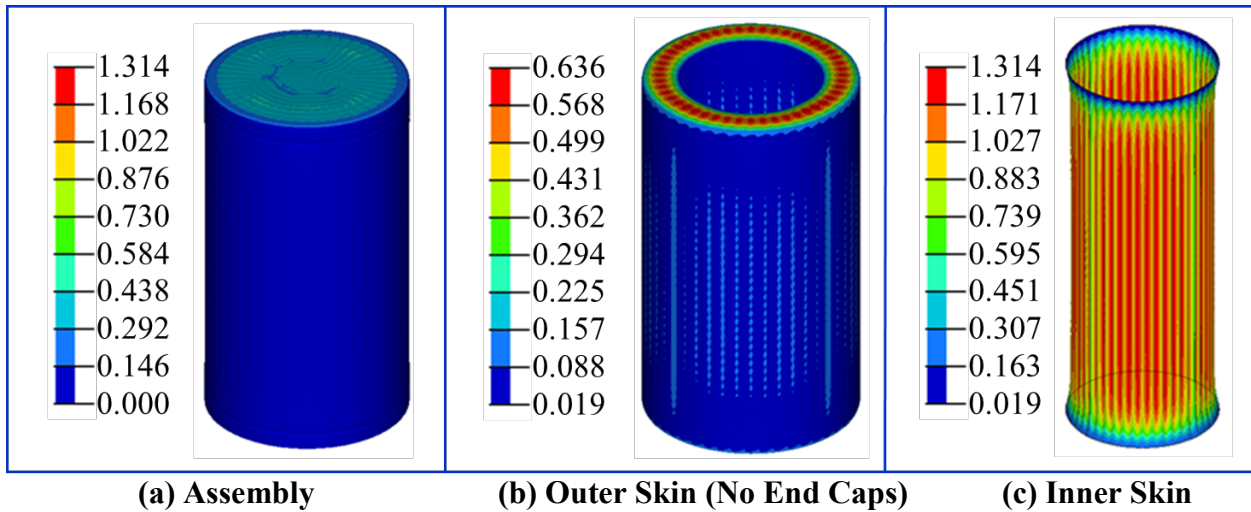


Figure 15. Displacements (Inches) of the Cylindrical PCQS Concept at 15.0 psig

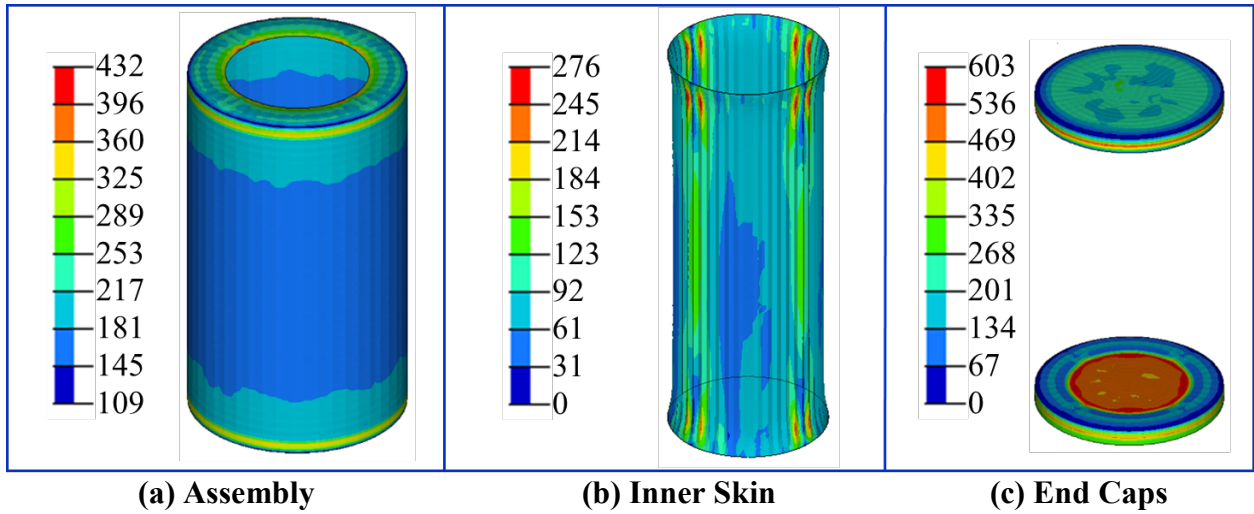


Figure 16. Tension-Running Loads (lbf/in.) for the Cylindrical PCQS at 15.0 psig

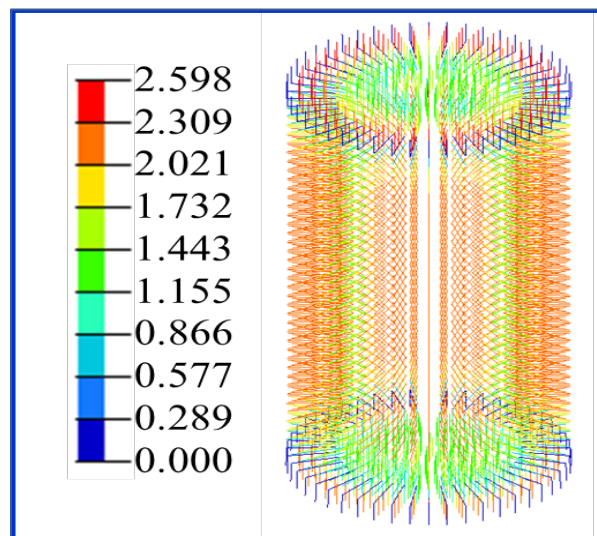


Figure 17. Drop-Yarn Tension Force (lbf) of the Cylindrical PCQS Concept at 15.0 psig

The influence of material extensibility of the cylindrical wall, roof, and floor panel skins and drop yarns on the individual component air volumes is shown in figure 18 as a function of inflation pressure. Note that the observed volume increase for each component was nearly linear with increasing inflation pressure.

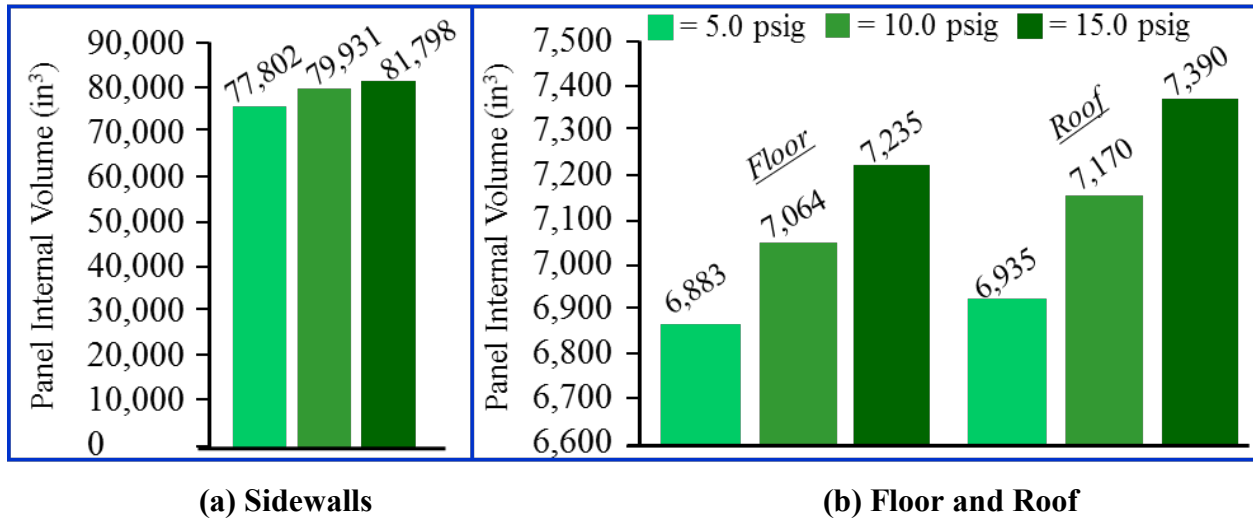


Figure 18. Air Volumes as a Function of Inflation Pressure for the Cylindrical PCQS Concept

The ergonomics of the cylindrical concept did not provide an acceptable and uniform standoff distance around the crew member, which was expected to infringe upon occupant comfort levels. Referring to figure 19 and considering the general dimensional parameters of a crew member, the ratio of shoulder width (lateral direction)-to-depth (ventral-to-dorsal direction) B/G and the ratio of height to total reach span A/F are key parameters. The diameter of the circular cylinder concept $D_{cylinder}$ is clearly driven by the shoulder width dimension G . The ventral/dorsal standoff distance is much greater than the lateral standoff distance; both are dependent on $D_{cylinder}$. The B/G aspect ratio suggests that a rectangular rather than cylindrical PCQS concept would provide improved ergonomics and comfort by allowing independent specification of the lateral and ventral/dorsal standoff distances. Additionally, the rectangular concepts, constructed with individual side and end drop-stitch panels, readily achieve tension and static equilibrium in both the inner and outer skins of the drop-stitch material components while maintaining uniform wall thickness with increasing inflation pressure. The multiple drop-stitch components of the rectangular PCQS concept better serve the redundant role as water storage bags because of their flat shapes for stackability and stowage when empty. The cylindrical drop-stitch component of the cylindrical PCQS concept does not provide for efficient water storage bag use, stackability, and stowage when empty.

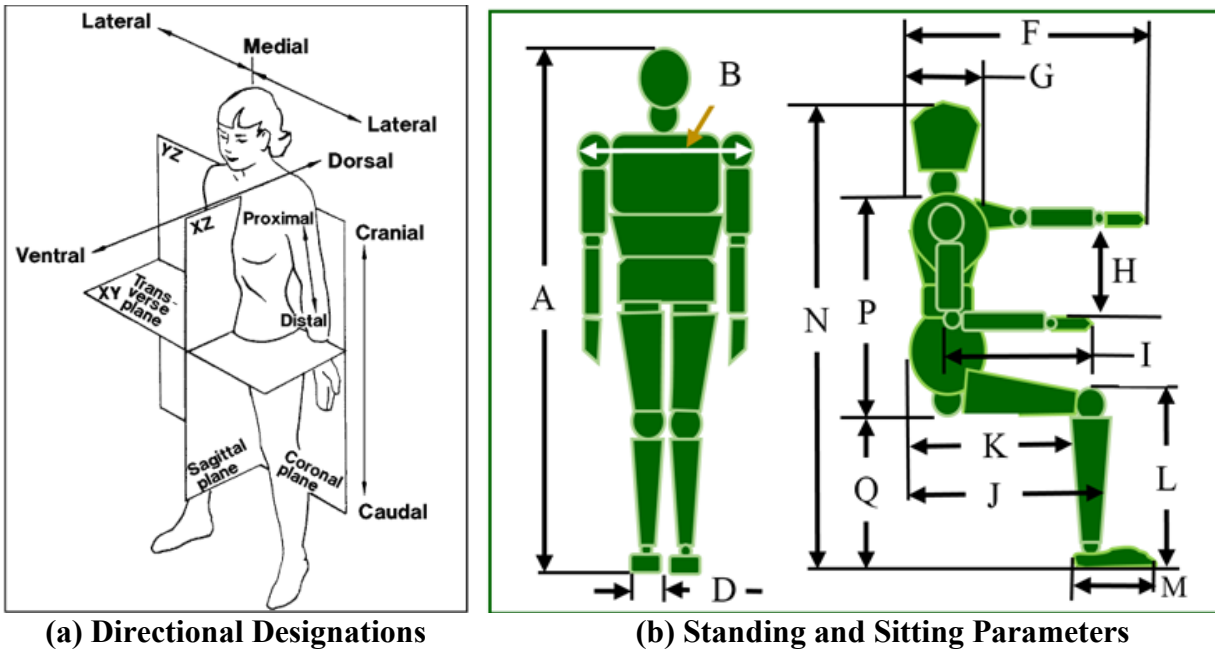
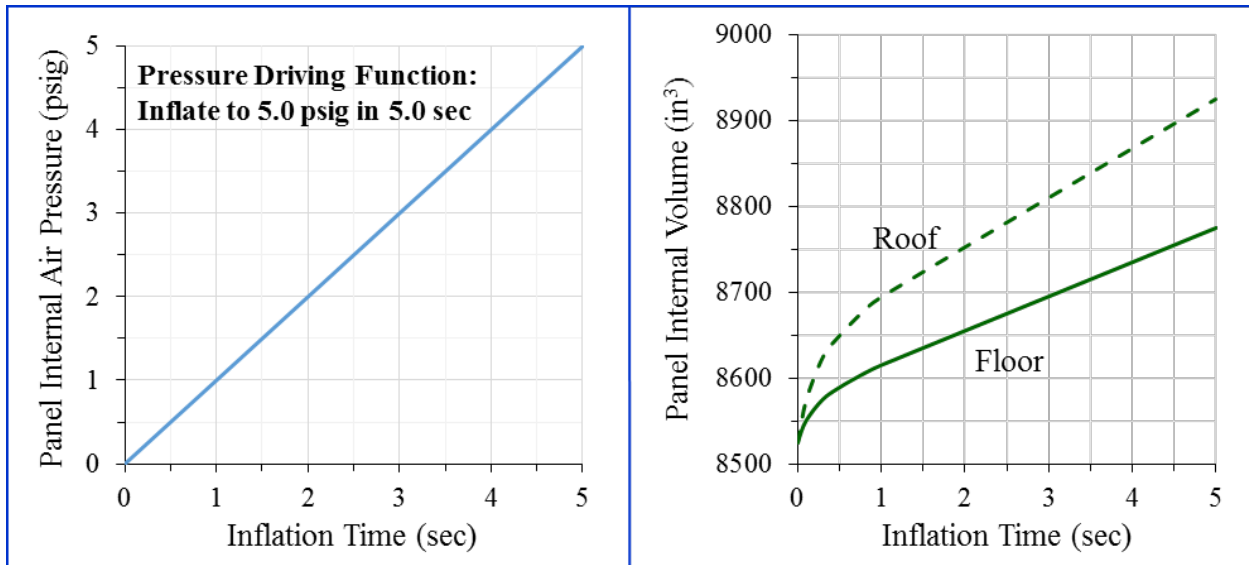


Figure 19. Definitions of Ergonomic (a) Planes and Directions¹⁸ and (b) Dimensions¹⁹

RECTANGULAR PCQS WITH INNER MEMBRANE LINER FEA MODEL

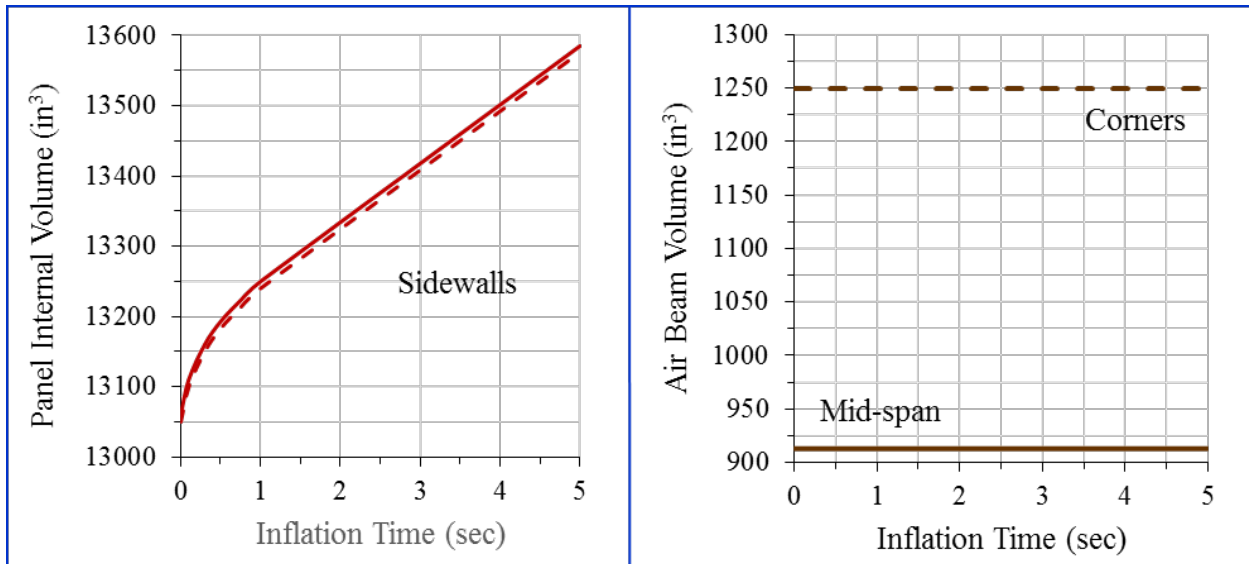
The rectangular PCQS (figure 2) has a rectangular framework arranged by a fabric skin/air-beam skeletal system that serves as the mounting frame for attaching the drop-stitch fabric panels (floor, roof, and sidewalls) with Velcro fasteners. The skeletal framework provides an air-cushioning support layer for crew comfort. The air beams are connected to the inner membrane layer and then inflated with air. Next, the individual drop-stitch fabric panels are filled with water and then mounted to the framework using Velcro fasteners. Ingress and egress is easily performed by connecting/disconnecting the Velcro fasteners.

Finite element results for this PCQS concept with the inner membrane liner (IML) are shown in figures 20–23. Note again that the drop-stitch fabric panels were inflated with air and were not filled with water. Fixed displacement boundary conditions were assigned to the floor panel’s bottom surface nodes. The pressure-driving functions for each compartment volume (that is, drop-stitch fabric panels and air beams) are shown in the upper left pressure-time history plot in figure 20. The remaining plots in figure 20 are the volume-time histories for each compartment. Note that beyond the 1.0-psi inflation pressure, the volume-time histories for the drop-stitch panels and air beams increased at a nearly constant rate. The displacement boundary conditions caused a difference in the inflated volumes of the floor and roof panels: specifically, the floor panel resulted in a volume increase (2.2%) smaller than that of the roof panel (2.9%). Because the four drop-stitch sidewall panels were identical in construction and attachment restraints, they each exhibited identical volume increases of 4.0%. Minimal volume changes (< 0.1%) were observed for the corner and mid-span air beams. These results include the FSI effects: the textile materials stretch and deform with increasing pressure leading to volume changes.



(a) 5.0 psig in 5.0 sec

(b) Roof and Floor Responses



(c) Sidewalls

(d) Air Beams

Figure 20. Rectangular PCQS Concept Responses with IML Pressurized to 15.0 psig

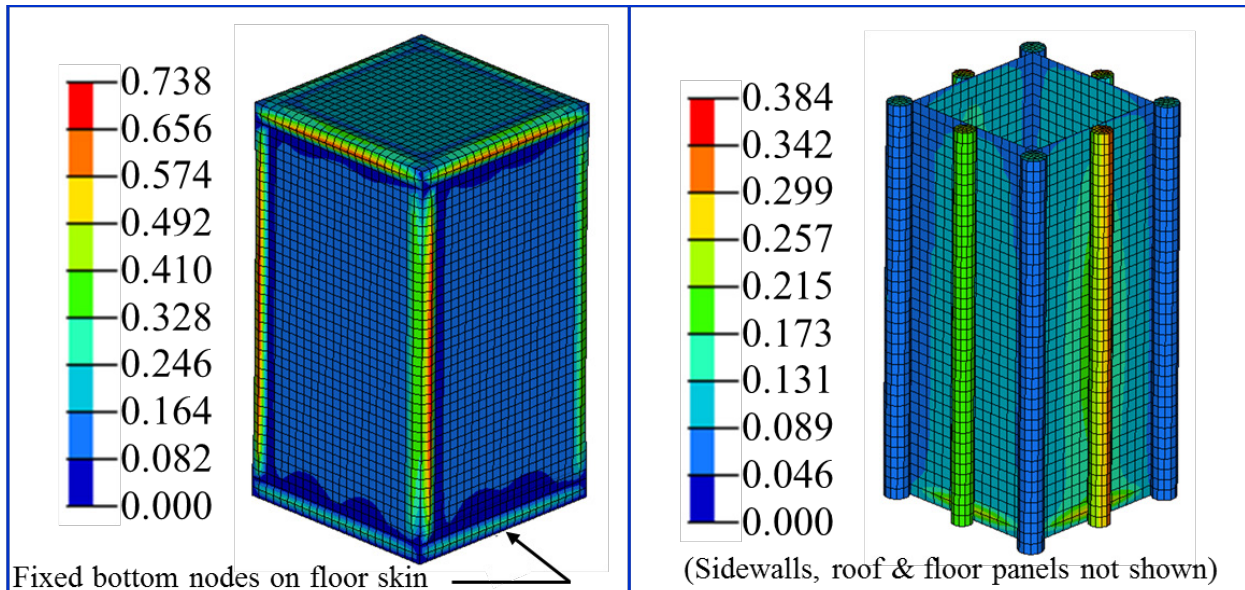
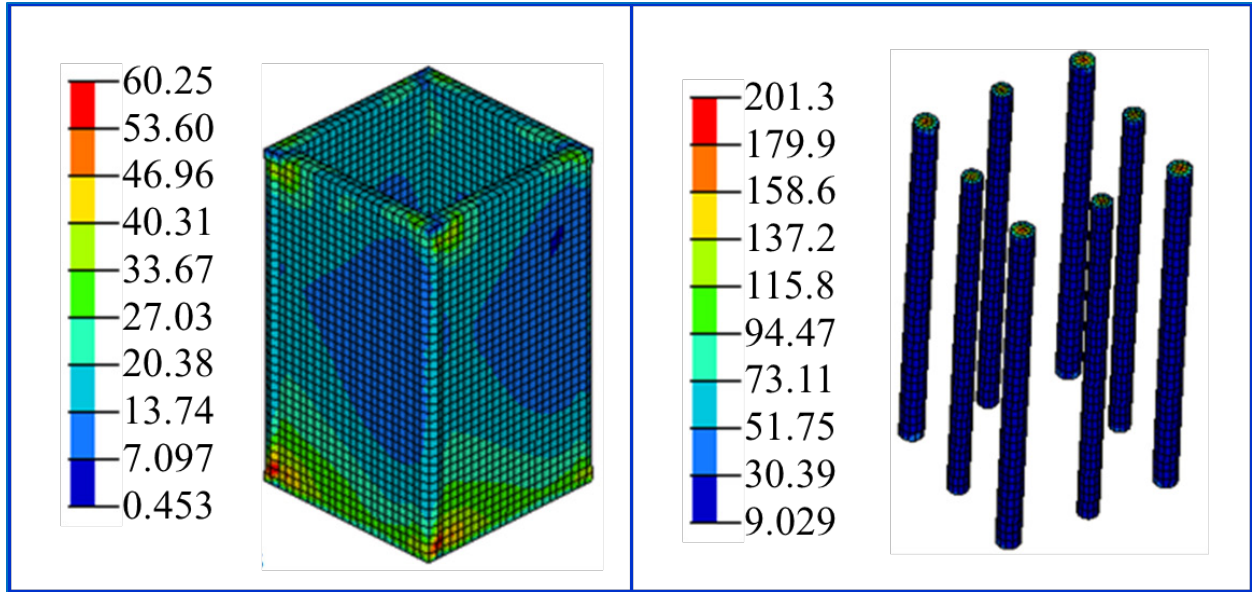


Figure 21. Displacements (Inches) of Rectangular PCQS Concept with IML at 5.0 psig

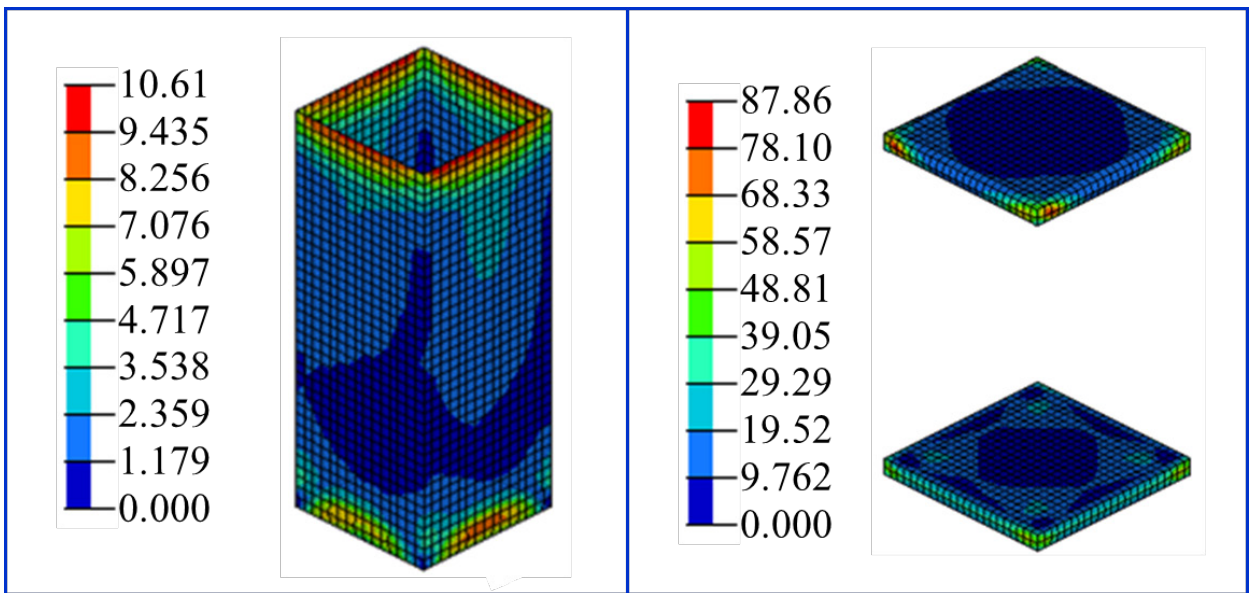
The resultant displacement contours shown in figure 21 demonstrate slight ballooning of the outer drop-stitch fabric skin layers (<0.75 in.) as expected. The reinforcement effects provided by the adjacently connected panels restricted the deflections along the panel edges. The reinforcement effects provided by the adjacently connected panels restricted the sidewall deflections; they shifted the region of maximum deformation away from the centers of the sidewalls. Deformations of the inner membrane and air beams are shown in the right-hand plot of the resultant displacement contours in figure 21. Deflections of the inner sidewall skins exhibited no waffling deformations, unlike the response of the circular PCQS concept.

Skin tensions per unit length (running loads) in the fabric components are shown in figure 22 and were relatively low. Peak values for each drop-stitch fabric panel were localized to adjacent edge regions. The overall maximum skin tension force per unit length was 201.3 lbf/in. developed in the end caps of the corner air beams. The tensile force in the drop yarns was 0.84 lbf as shown in figure 23. This PCQS concept exhibited no deployment issues because the air beams and IML remained straight and flat for the 5.0-psig inflation pressure.



(a) Sidewall Skins

(b) Air Beams



(c) IML

(d) Roof and Floor Sections

Figure 22. Tension-Running Loads (lbf/in.) with IML at 5.0 psig

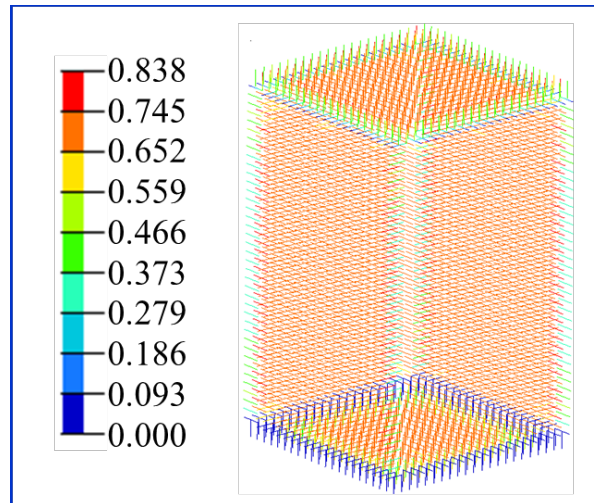


Figure 23. Drop-Yarn Tension Force (lbf) with IML at 5.0 psig

Results of the rectangular PCQS concept with IML at inflation pressures of 10.0 and 15.0 psig are shown in figures 24–31.

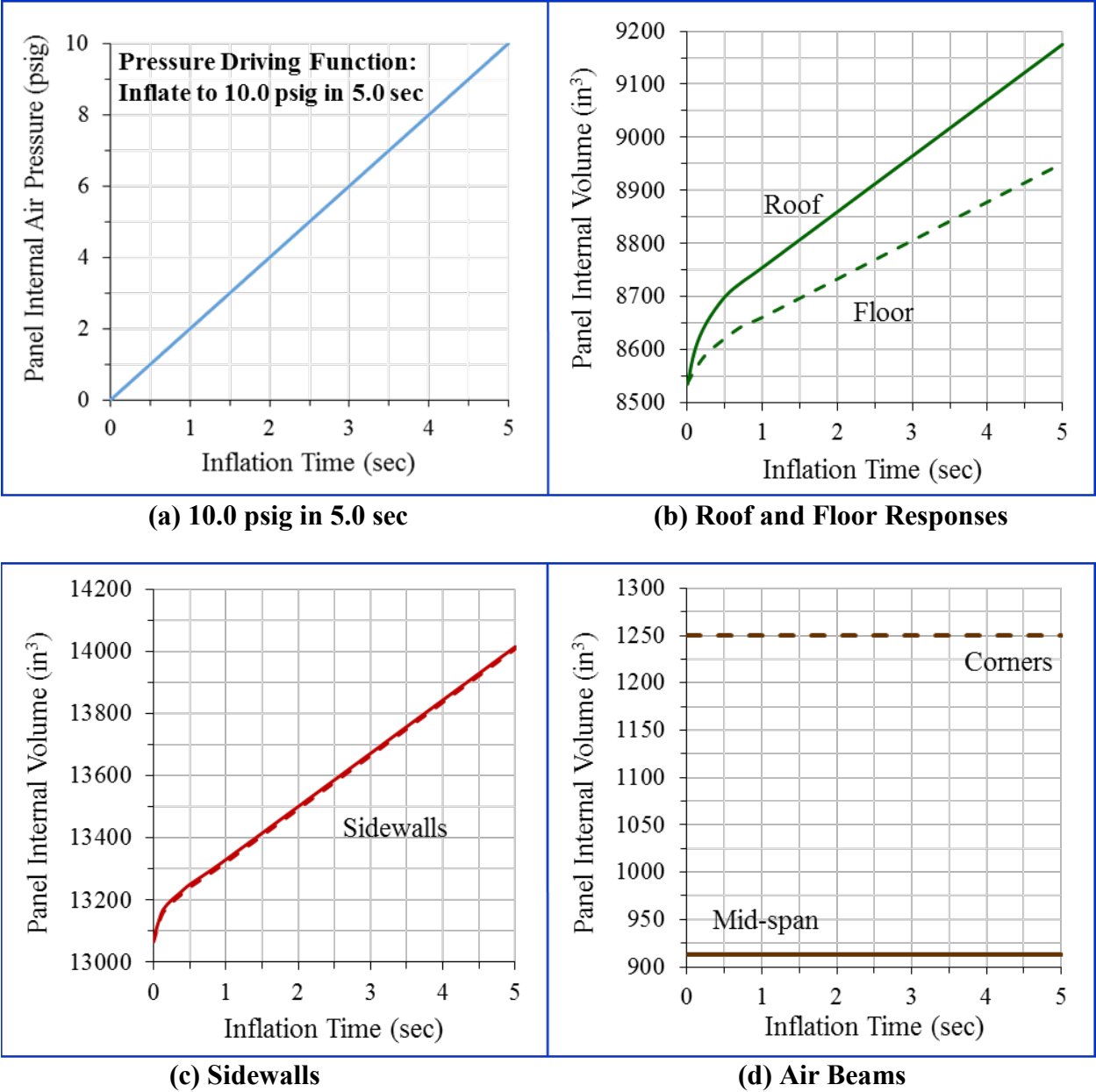


Figure 24. Rectangular PCQS Concept Responses with IML Pressurized to 10.0 psig

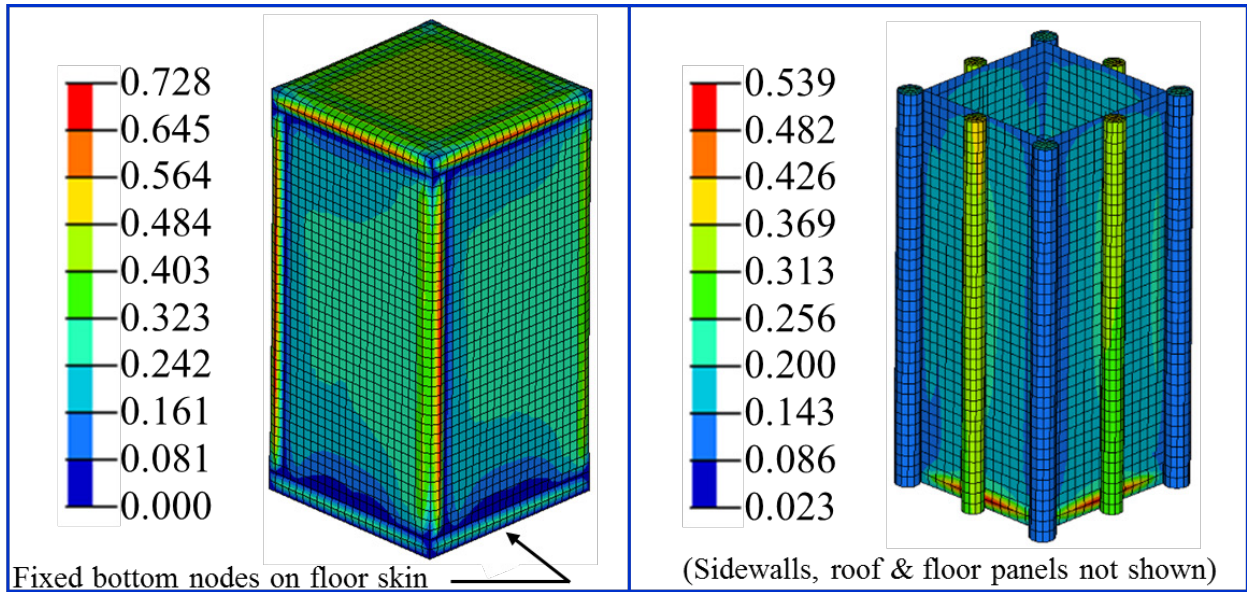


Figure 25. Displacements (Inches) of Rectangular PCQS Concept with IML at 10.0 psig

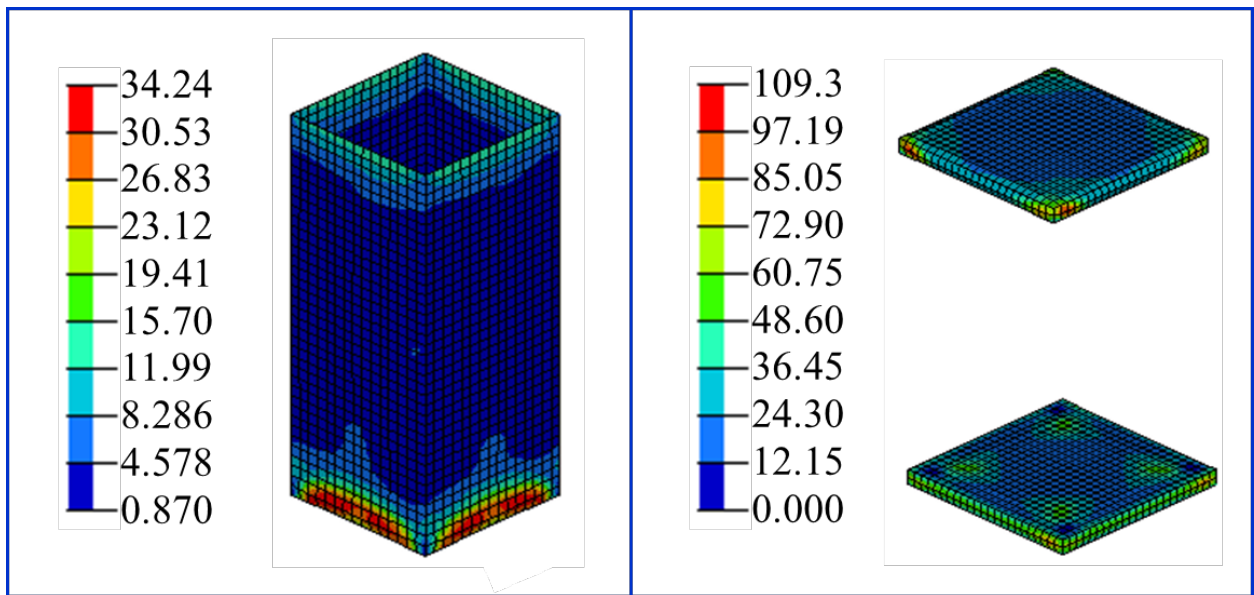
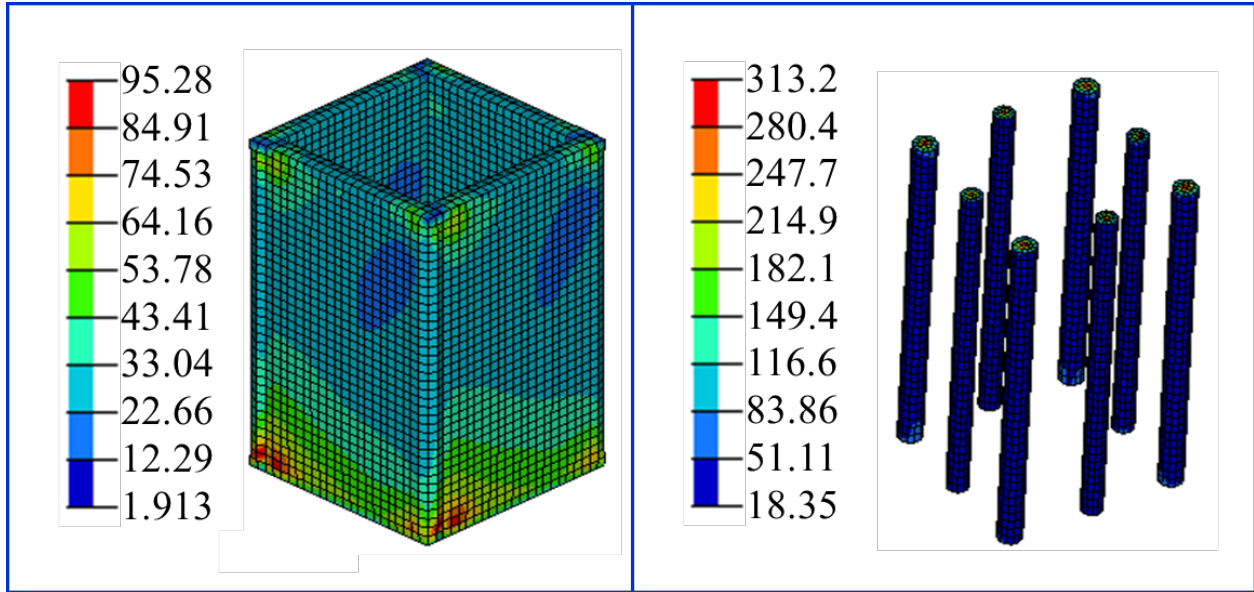


Figure 26. Tension-Running Loads (lb/in.) with Rectangular PCQS Concept IML at 10.0 psig

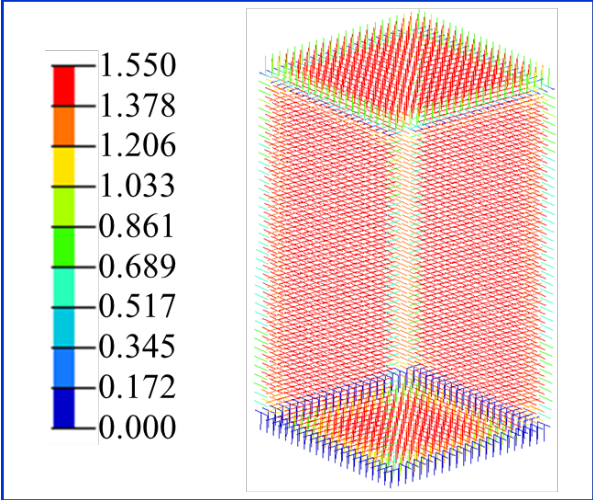
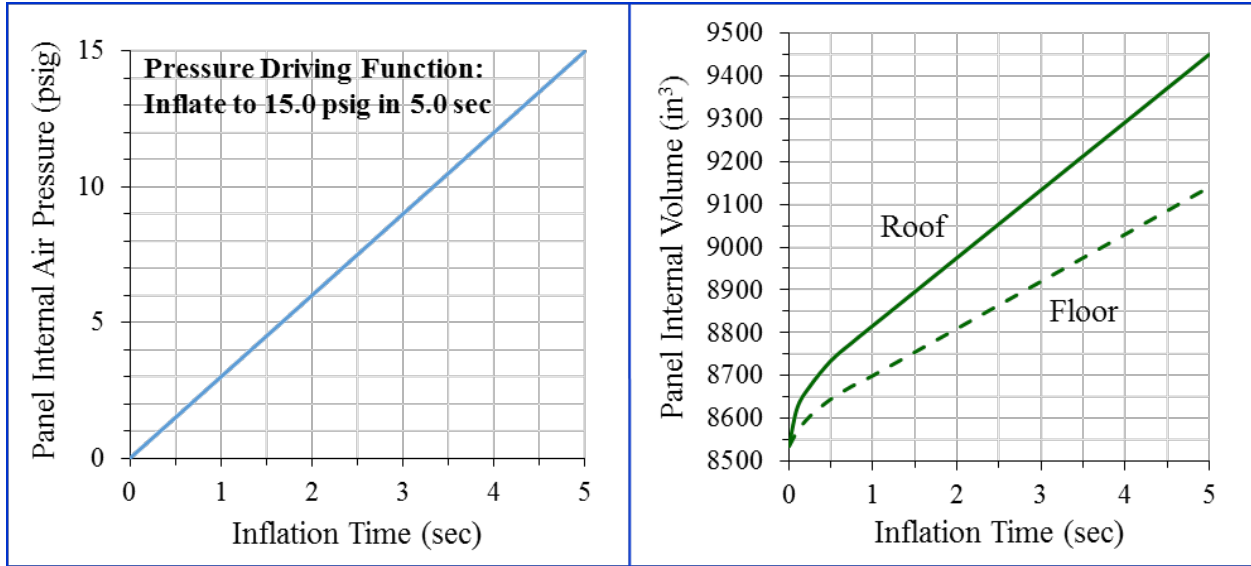
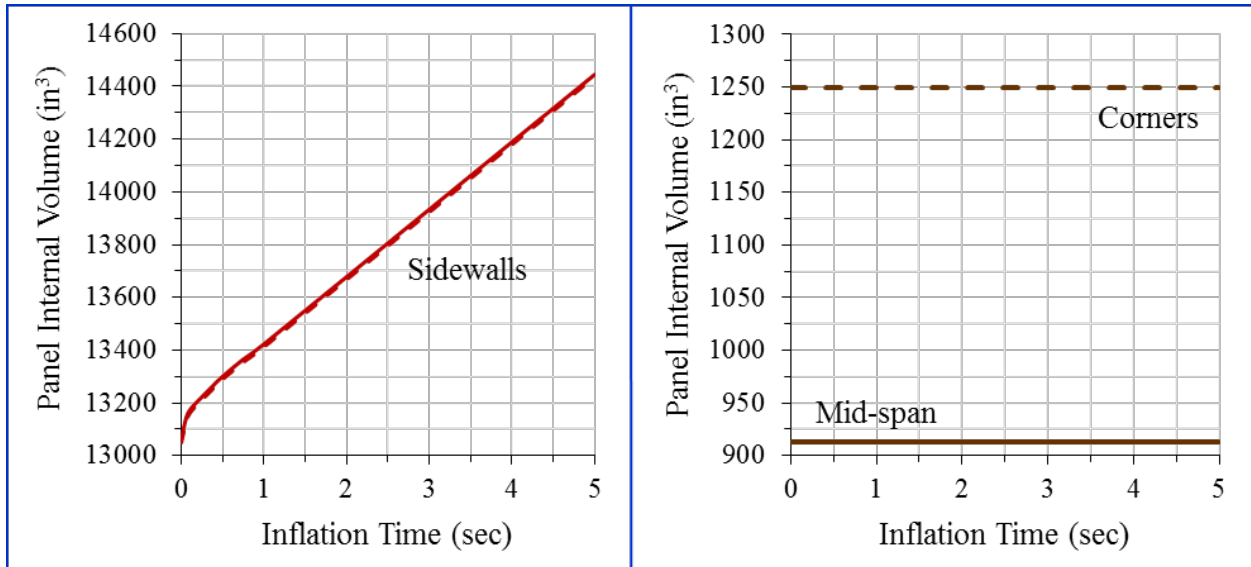


Figure 27. Drop-Yarn Tension Force (lbf), Rectangular PCQS Concept with IML at 10.0 psig



(a) 10.0 psig in 5.0 sec

(b) Roof and Floor Responses



(c) Sidewalls

(d) Air beams

Figure 28. Rectangular PCQS Concept Responses with IML Pressurized to 15.0 psig

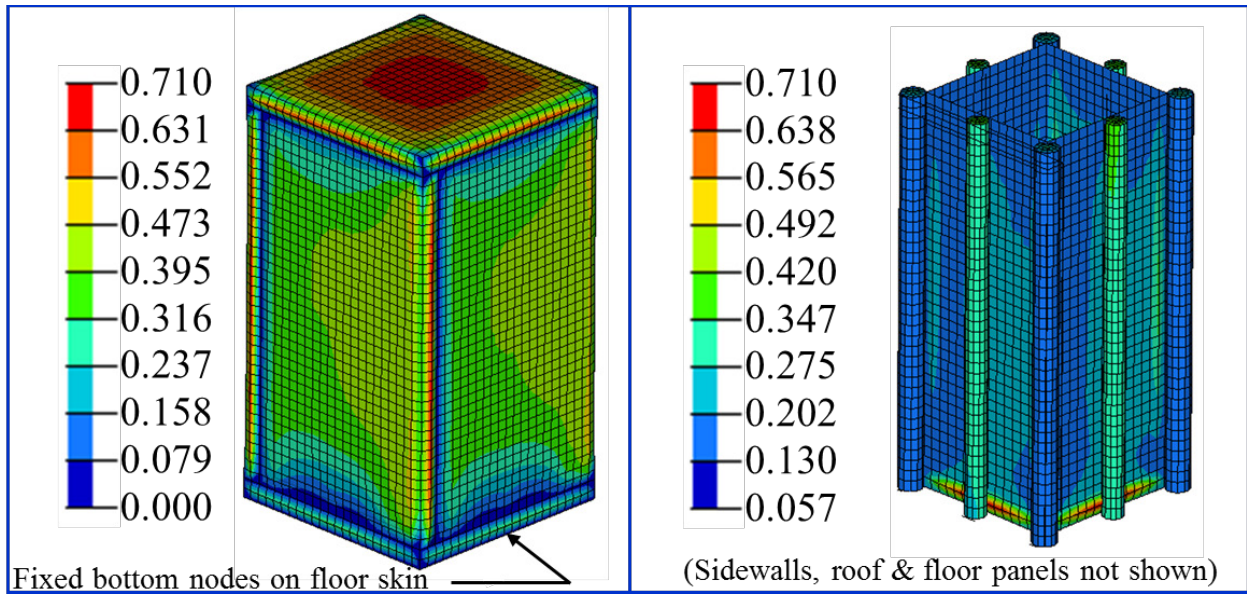


Figure 29. Displacements (Inches) of Rectangular PCQS Concept with IML at 15.0 psig

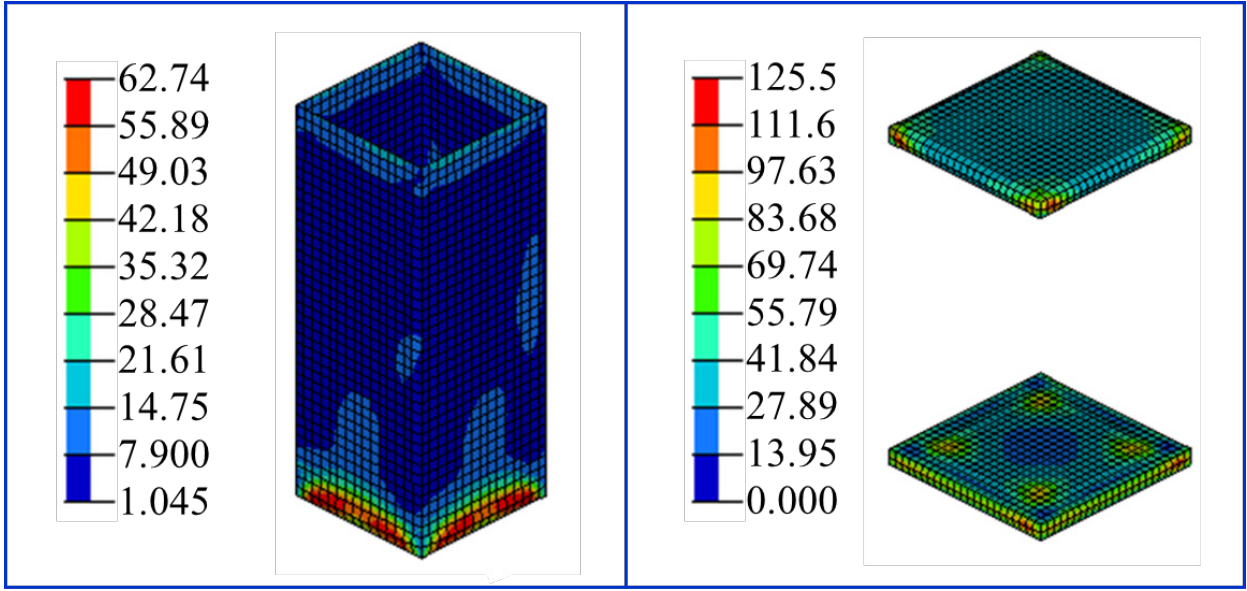
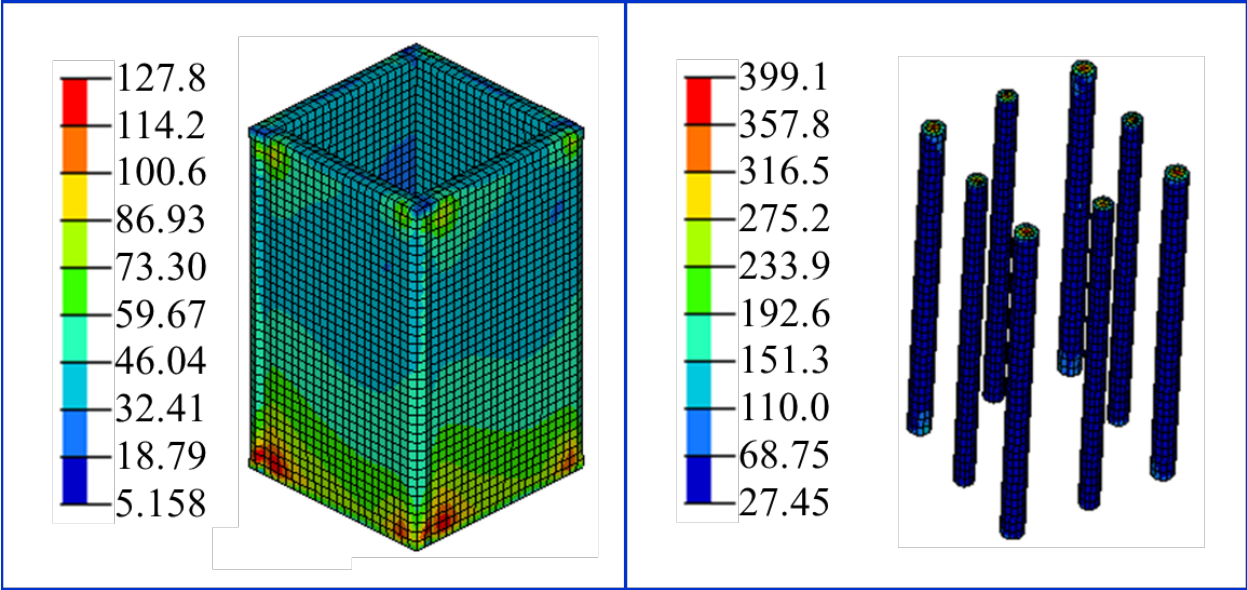


Figure 30. Tension-Running Loads (lb/in.) with Rectangular PCQS Concept IML at 15.0 psig

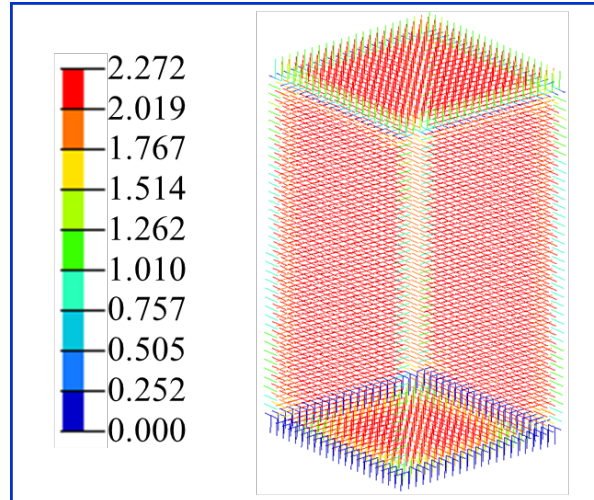


Figure 31. Drop-Yarn Tension Force (lbf), Rectangular PCQS Concept, IML at 15.0 psig

The volumes for each inflatable component are listed in table 2 as functions of inflation pressure and are plotted in figure 32.

Table 2. Component Air Volumes of the Rectangular PCQS Concept with Inner Membrane Liner

Inflation Pressure (psig)	Volume (in. ³)				
	Sidewall	Floor	Roof	Corner Air Beam	Mid-Span Air Beam
5.0	13,579.7	8,776.4	8,921.7	1,252.5	913.0
10.0	14,006.7	8,952.1	9,182.1	1,252.9	913.4
15.0	14,443.3	9,135.1	9,452.0	1,253.1	913.5

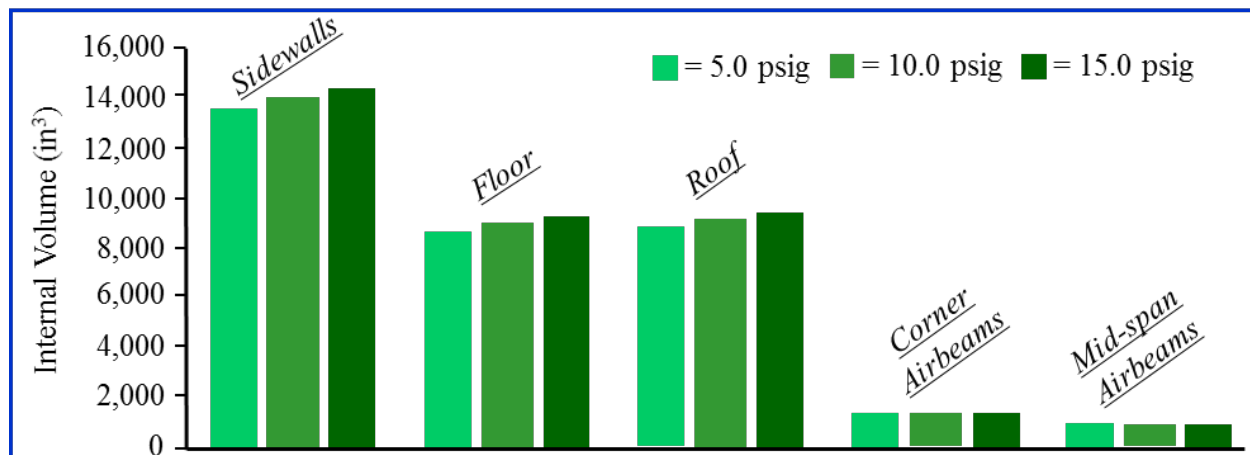


Figure 32. Air Volumes as a Function of Inflation Pressure, Rectangular PCQS Concept, with IML

The maximum skin tensions and drop-yarn forces for each inflation pressure are listed in table 3 and plotted in figure 33. Note that the maximum skin tensions for each component increased in a near-linear rate with increasing inflation pressure.

Table 3. Skin Tension Force per Unit Length Results of the Rectangular PCQS Concept with IML

Inflation Pressure (psig)	Maximum Skin Tension (lbf/in.)				Maximum IML (lbf/in.)
	Sidewall	Floor	Roof	Air Beam	
5.0	60.25	65.2	87.9	201.3	10.6
10.0	95.3	95.5	109.3	313.2	34.2
15.0	127.8	125.5	122.5	399.0	62.7

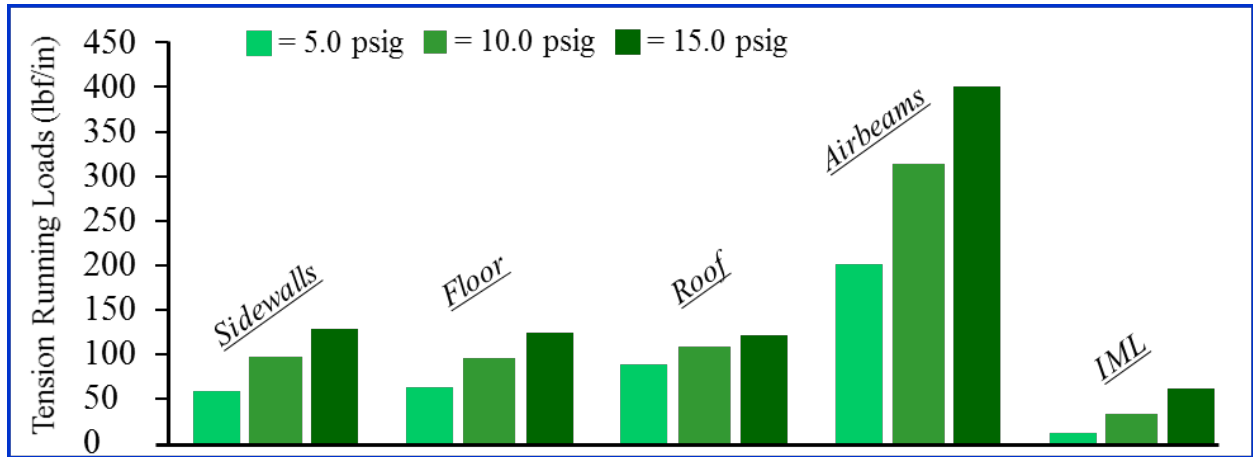


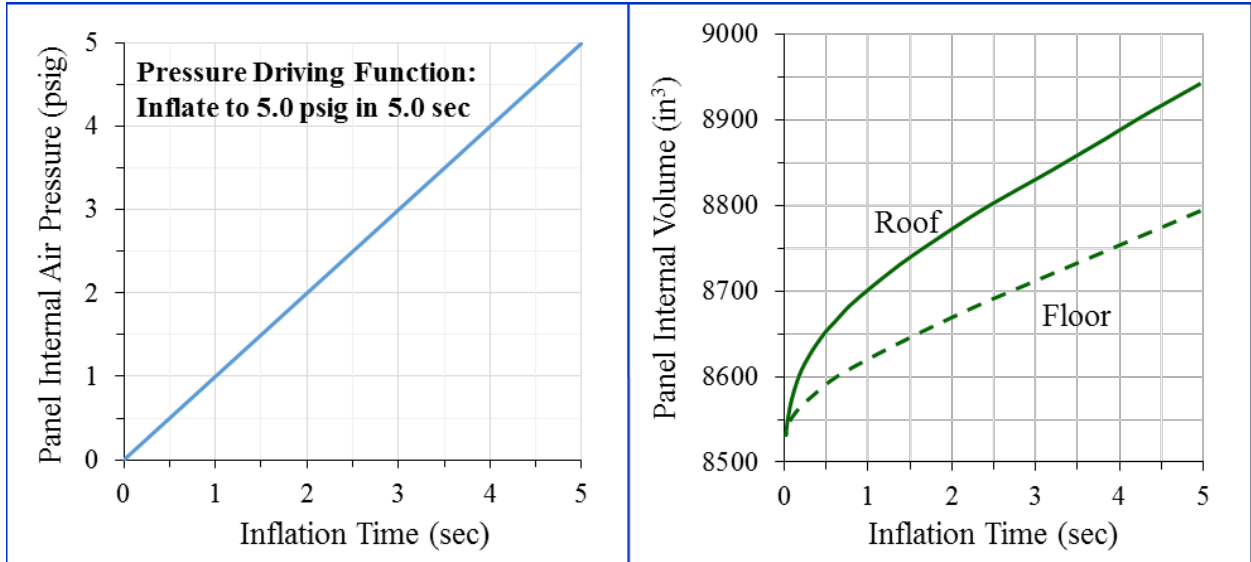
Figure 33. Peak Tension-Running Loads (lbf/in.) Versus Pressure, Rectangular PCQS Concept, with IML

RECTANGULAR PCQS WITH EMBEDDED AIR BEAMS FEA MODEL

A second rectangular PCQS concept was considered as a modified version of the previous rectangular concept (rectangular PCQS with inner membrane liner). Here, the inner drop-stitched section was removed to accommodate the vertical air beams that were embedded within the drop-stitch fabric panels along the panel's vertical edges. Otherwise, the drop-stitched fabric remained pristine. The air beams of this concept were initially filled with air for deployment purposes, and, once the drop-stitch fabric panels were filled with water, the air in the air beams was released and replaced with water to enable full operational use of the enclosure.

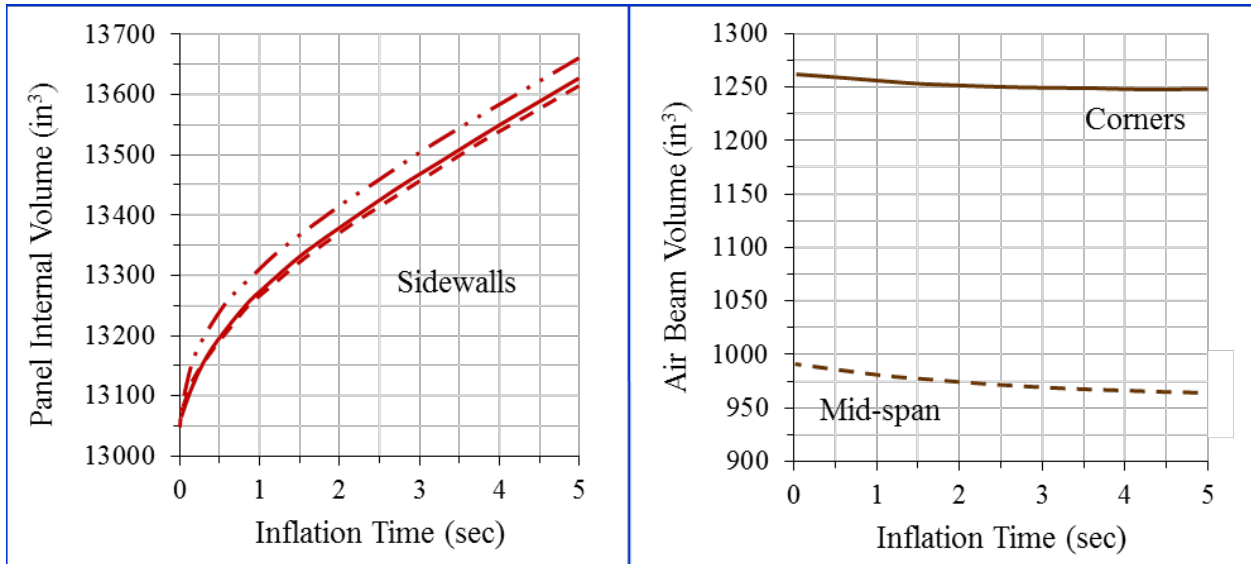
The pressure and volume time-histories for each compartment are plotted in figure 34 for the 5.0-psig inflation case. The effects of the displacement boundary conditions on the bottom surface of the floor panel resulted in the different inflated volumes of the floor and roof panels (see figure 34(b)); this effect was the same as that observed for the previous rectangular PCQS concept.

Contours of the resultant displacement magnitudes are shown in figure 35, with the largest value occurring along the edge of the roof panel (0.709 in.). The maximum stress resultants for each component were 201.3 lbf/in. for the air beams, 60.3 lbf/in. for the sidewalls, and 87.9 lbf/in. for the roof and floor panels combined, as shown in figure 36. The peak drop-yarn tension force was 0.97 lbf as shown in figure 37.



(a) 5.0 psig in 5.0 sec

(b) Roof and Floor Responses



(c) Sidewalls

(d) Air Beams

Figure 34. Rectangular PCQS Concept Responses with IML Pressurized to 5.0 psig

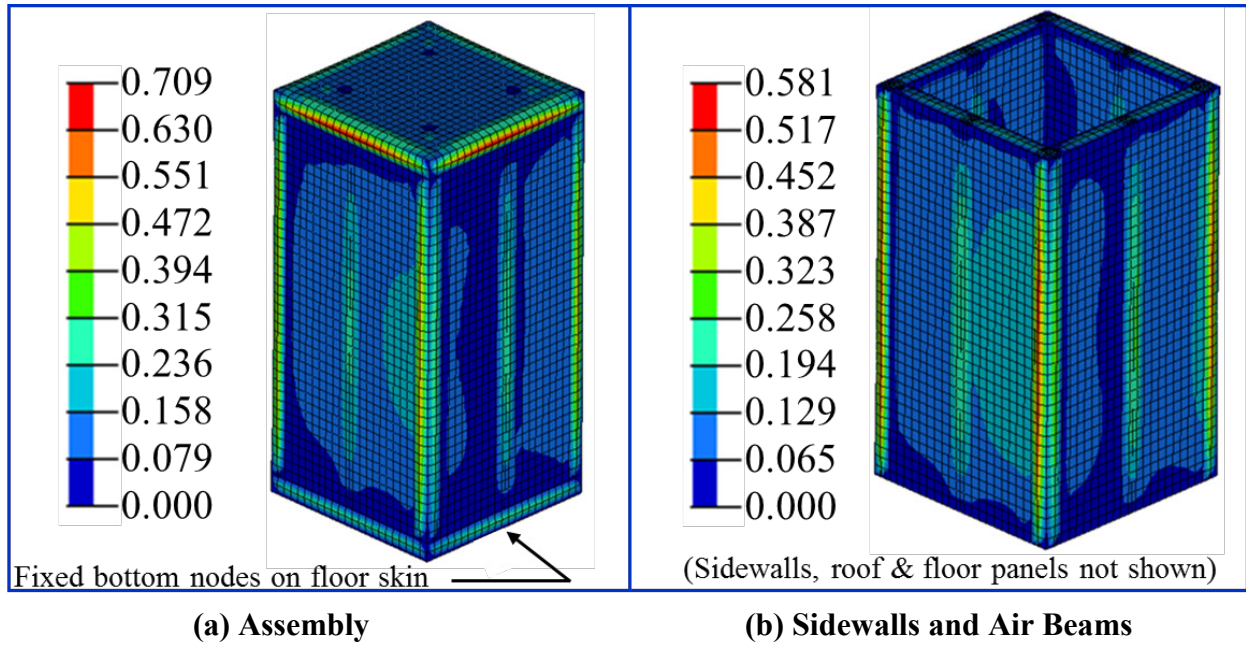
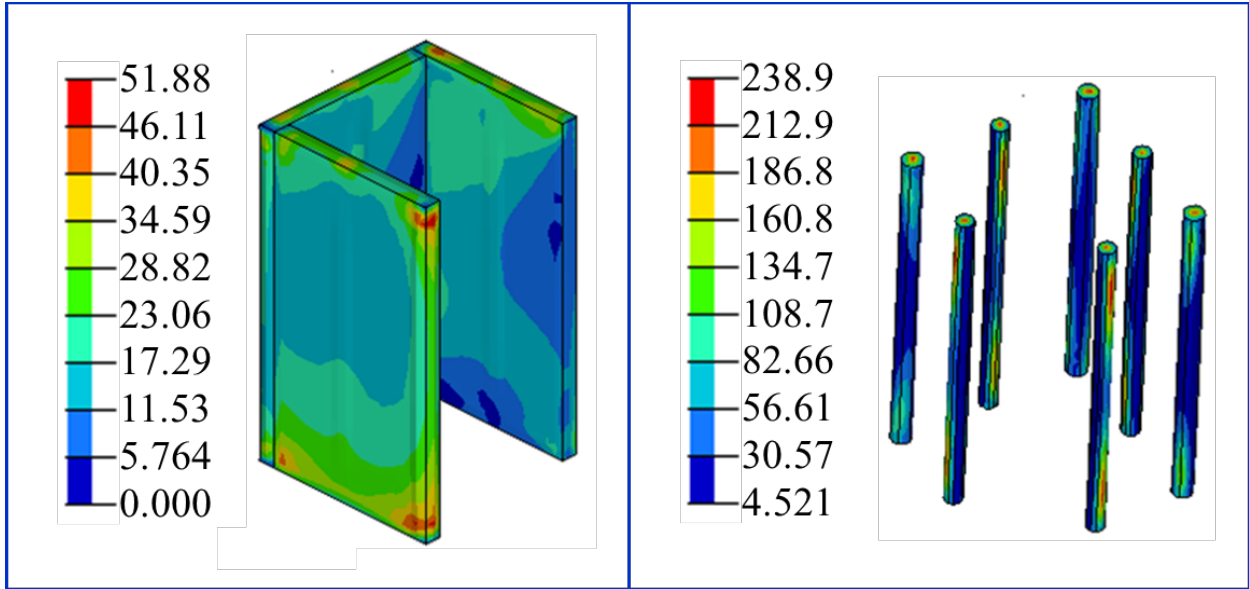
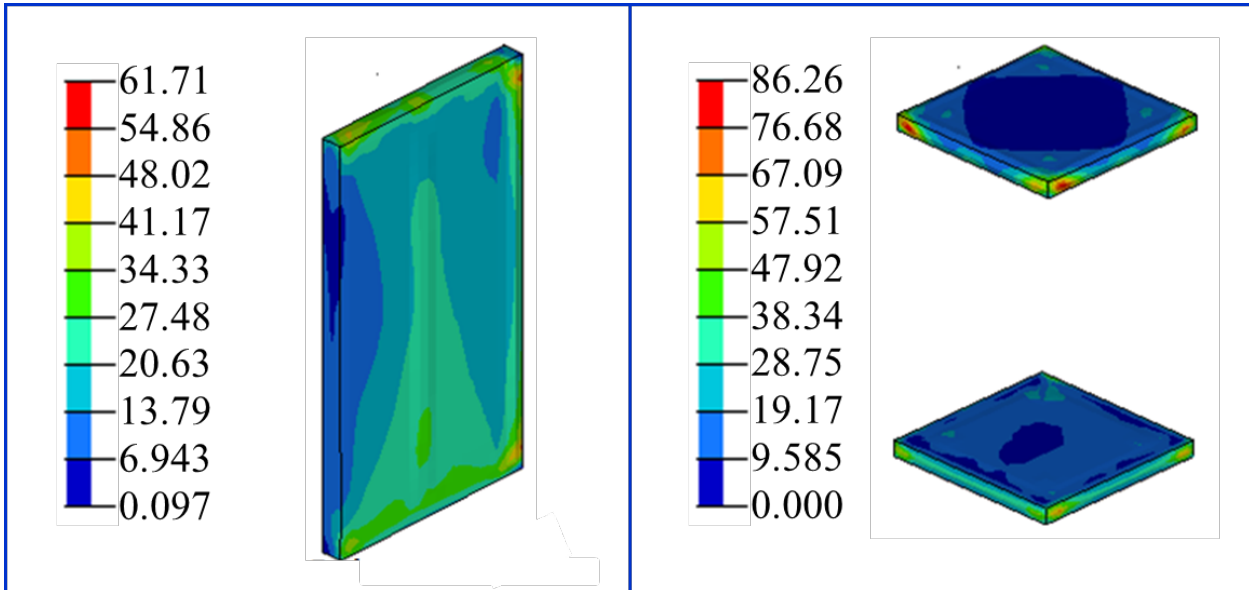


**Figure 35. Displacements (Inch), Rectangular PCQS Concept
(with Embedded Air Beams) at 5.0 psig**



(a) Three Sidewalls Without Embedded Air Beams

(b) Air Beams



(c) Rightmost Sidewall from (a)

(d) Roof and Floor Sections

Figure 36. Tension-Running Loads (lb/in.) with Rectangular PCQS Concept IML at 5.0 psig

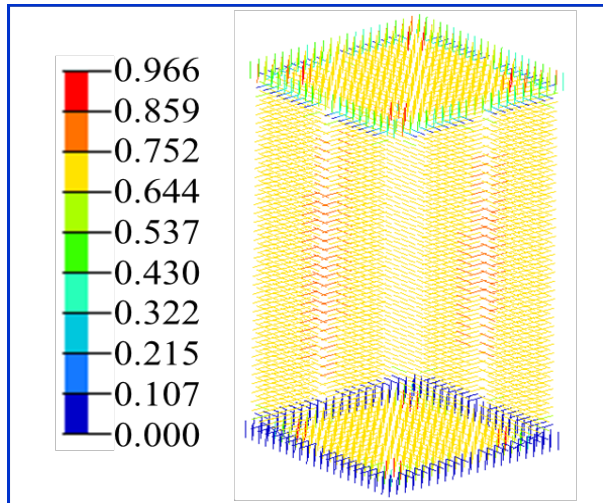
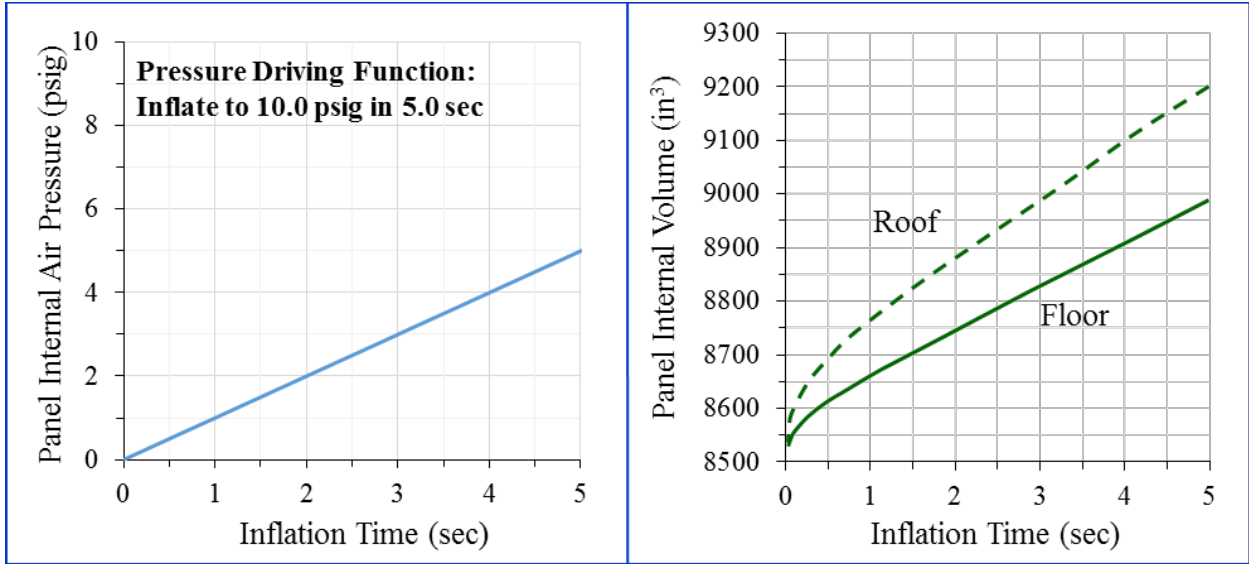


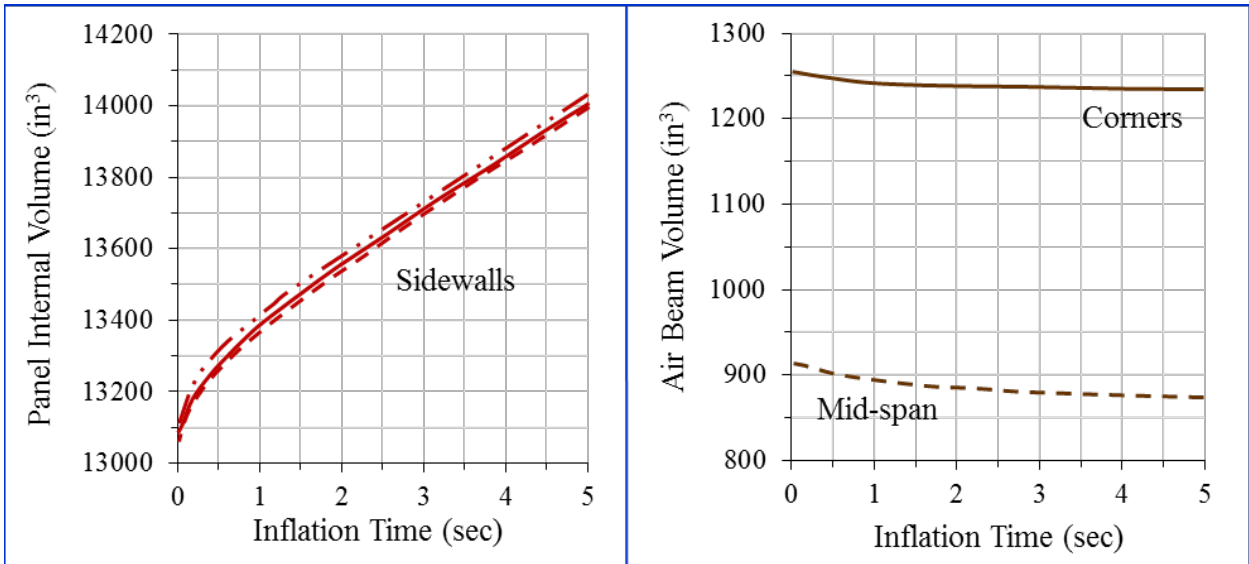
Figure 37. Drop-Yarn Tension Force (lbf) of the Rectangular PCQS Concept with IML at 5.0 psig

Results for the 10.0-psig inflation case were obtained for this concept and are shown in figures 38–41. Figure 38 shows the pressure and volume time histories for each compartment. The sidewall volumes at 10.0 psig were 2.7% greater than those observed for the 5.0-psig case. The roof and floor panel volumes increased by 2.3% and 1.8%, respectively, over the values corresponding to the 5.0-psig case. The air beam volumes, however, were observed to decrease by <4% from their initial (unpressurized) states with increasing inflation pressure as a result of constraining effects caused by the interacting sidewalls and roof and floor panels. The maximum resultant displacement occurred again along the edge of the roof panel and was less than 0.2% greater than that observed in the 5.0-psig case. Peak values of the skin tension force per unit length occurred in the air beams (364 lbf/in.); the next highest value developed in the roof and floor panels (128 lbf/in.), followed by the right sidewall (96 lbf/in.). Peak drop-yarn tension forces were 1.86 lbf and were observed in the roof and floor panels at locations above (roof) and below (floor) the corner air beams.



(a) 10.0 psig in 5.0 sec

(b) Roof and Floor Responses



(c) Sidewalls

(d) Air Beams

Figure 38. Rectangular PCQS Concept Responses (with Embedded Air Beams) Up to 10.0 psig

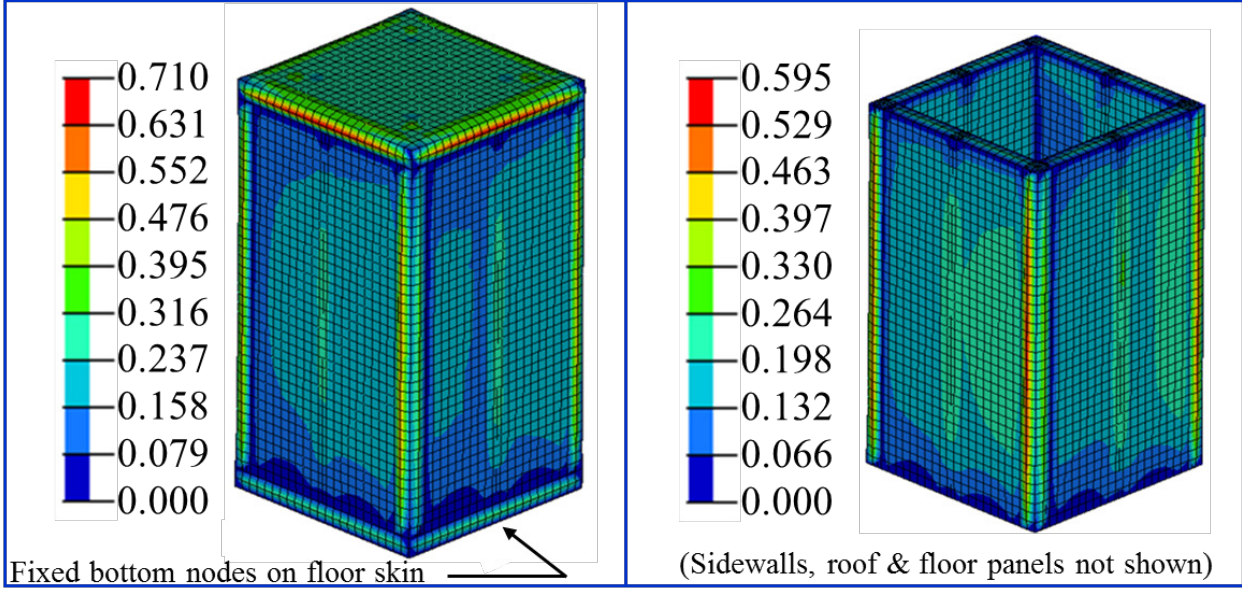
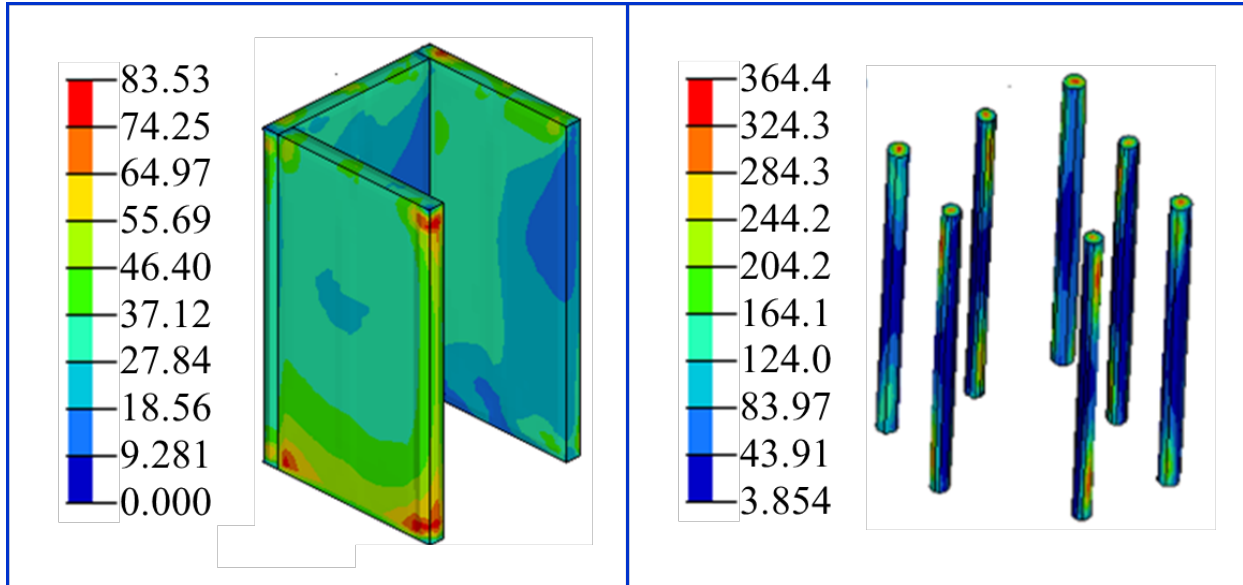
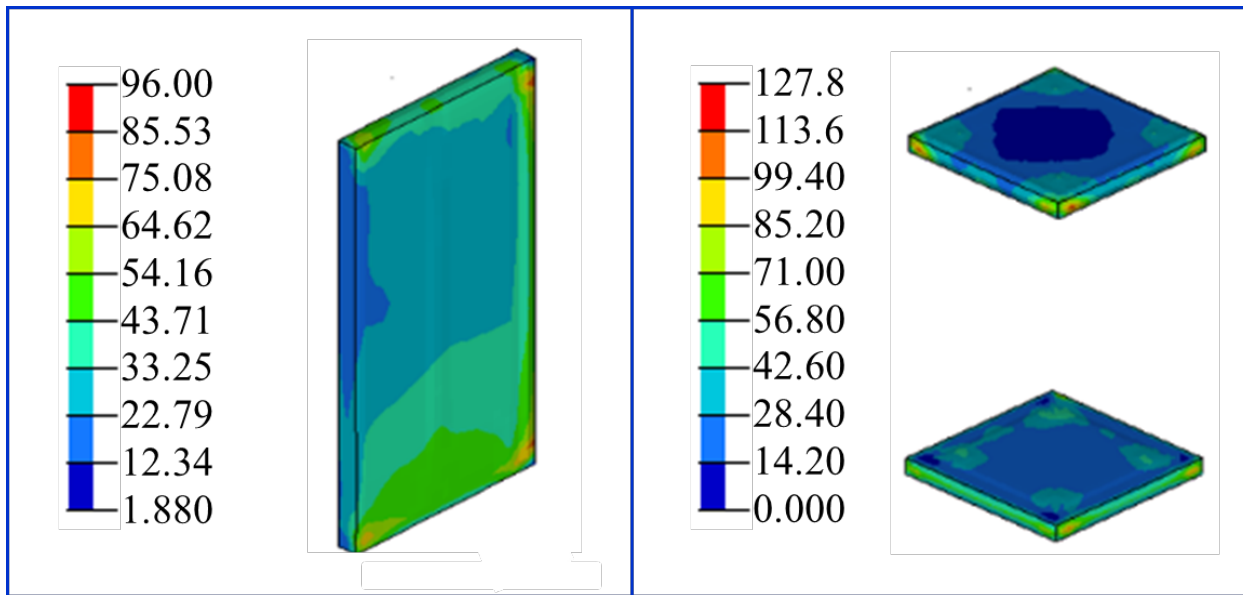


**Figure 39. Displacements (Inch), Rectangular PCQS Concept
(with Embedded Air Beams) at 10.0 psig**



(a) Three Sidewalls Without Embedded Air Beams

(b) Air Beams



(c) Rightmost Sidewall from (a)

(d) Roof and Floor Sections

Figure 40. Stresses (psi) of Rectangular PCQS Concept (with Embedded Air Beams) at 10.0 psig

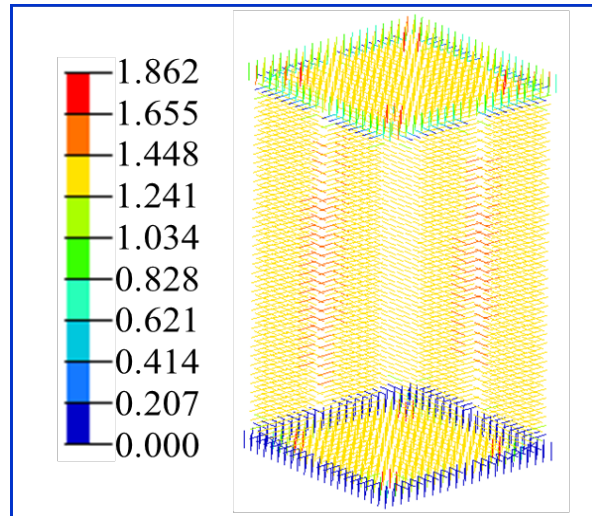
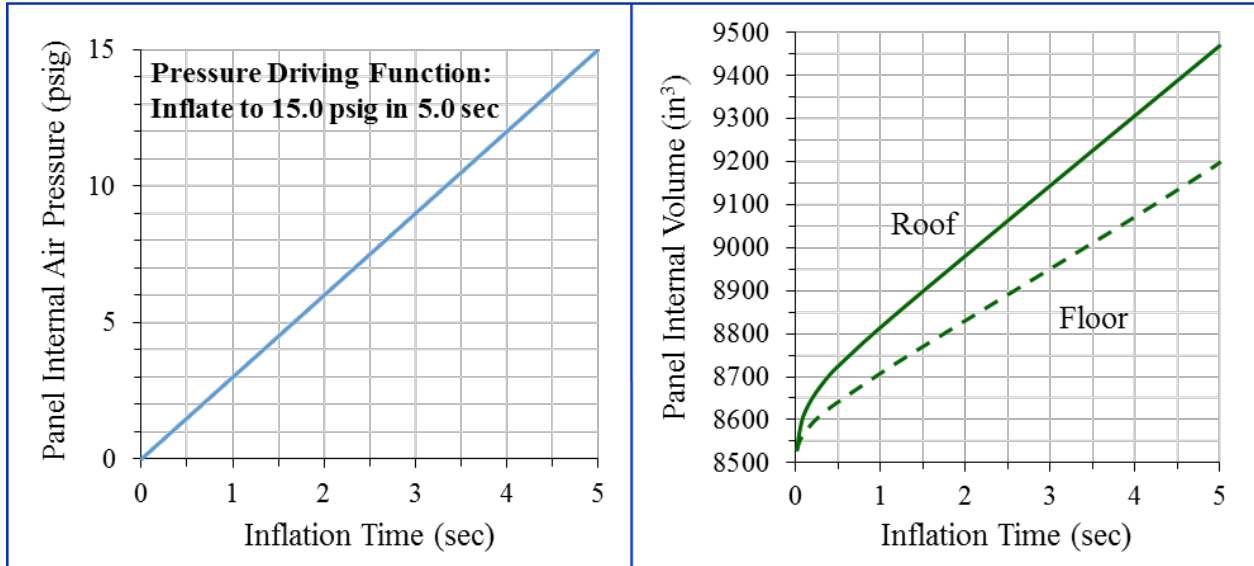


Figure 41. Drop-Yarn Tension Force (lbf) of PCQS Concept (with Embedded Air Beams) at 10.0 psig

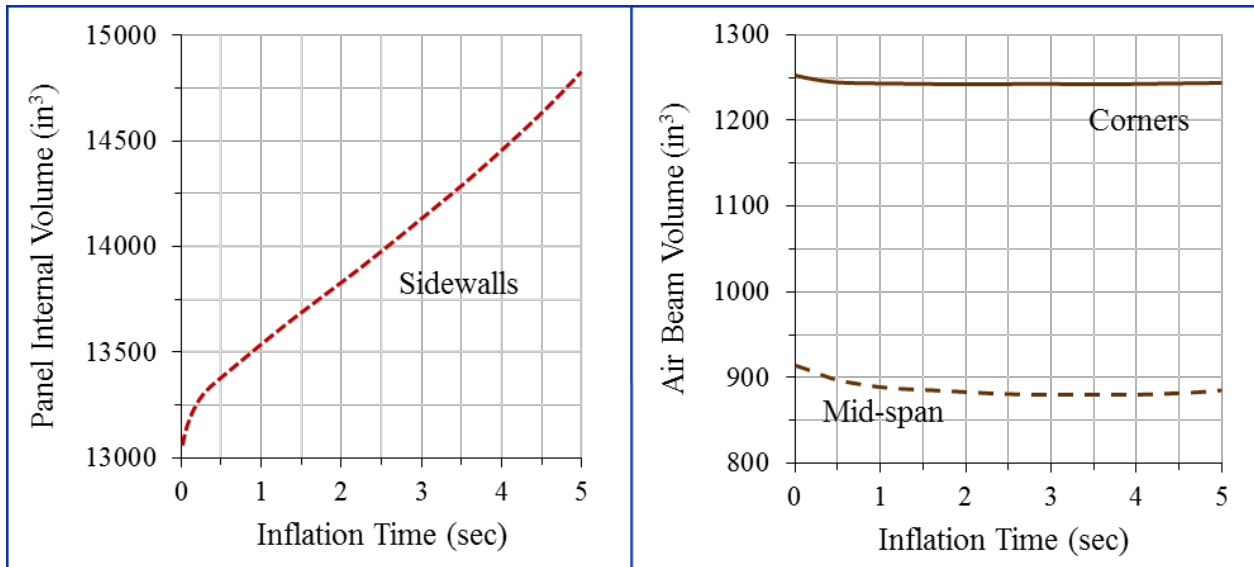
Results of the 15.0-psig inflation case are shown in figures 42–45. The pressure and volume time histories for each compartment are plotted in figure 42. A nominal increase in the sidewall volumes of 1.8% was observed over the corresponding 10.0-psig inflation case. The roof and floor panel volumes increased incrementally over the 10.0-psig case by 3.5% and 2.3%, respectively. The corner and mid-span air beam volumes increased by 1.1% and 0.7%, respectively, over those predicted for the 10.0-psig inflation case. As observed in the 10.0-psig inflation case, the constraining effects caused by the interacting sidewalls and roof and floor panels continued. For inflation pressures increasing beyond 12.0 psig, the air beam volumes began to increase; however, at 15.0 psig, the mid-span and corner air beam volumes were approximately 4% and 0.6% less, respectively, than their initial state (unpressurized) volumes.

The location of maximum resultant displacement shifted from the edge of the roof panel to the edge of the sidewall panels in the area surrounding the corner air beams—the result of the local removal of drop yarns within the sidewalls to accommodate the air beams. Peak values of the skin tension force per unit length occurred in the air beams (427 lbf/in.); the next highest value developed in the right sidewall (143 lbf/in.), followed by the roof panel (118 lbf/in.). Peak drop-yarn tension forces were 2.91 lbf and were observed in the roof and floor panels at locations above (roof) and below (floor) the corner air beams.



(a) 15.0 psig in 5.0 sec

(b) Roof and Floor Responses



(c) Sidewalls

(d) Air Beams

Figure 42. Responses for Rectangular PCQS Concept (with Embedded Air Beams) Up to 15.0 psig

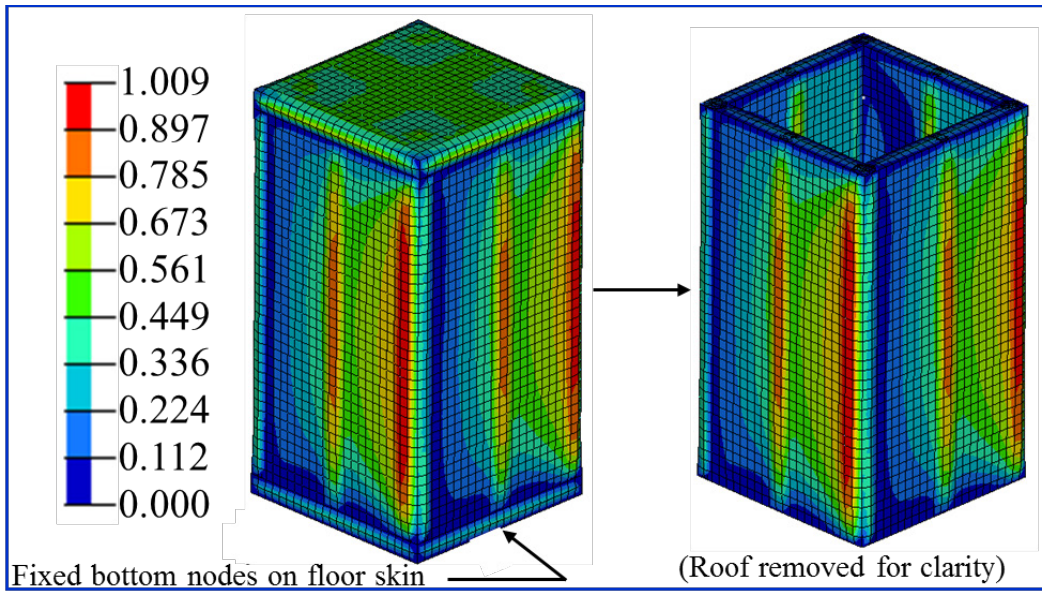
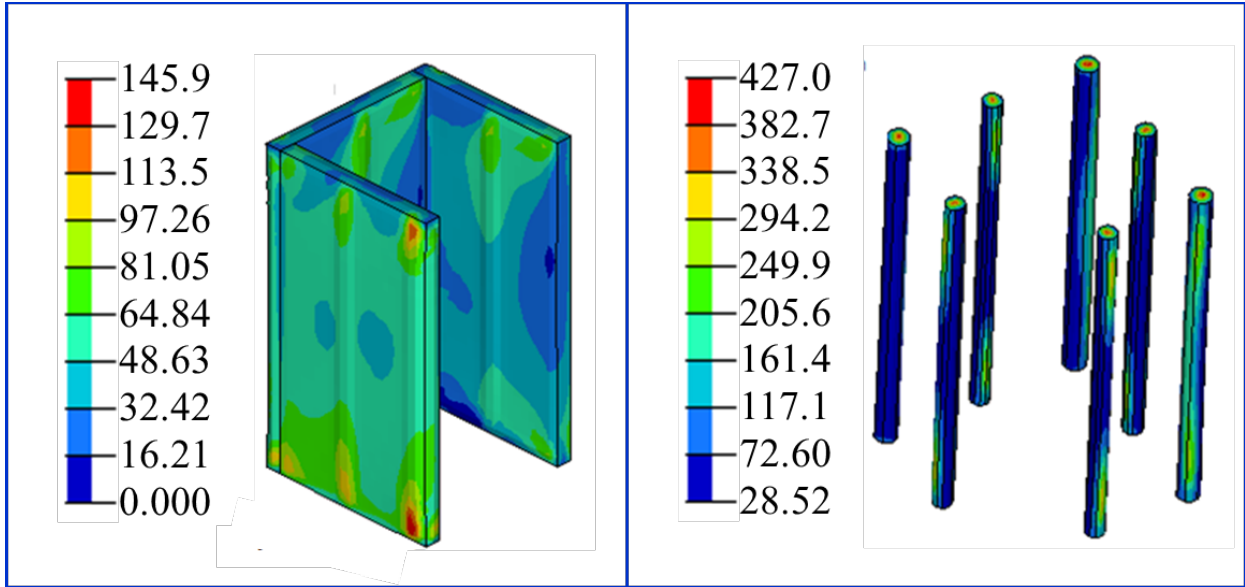
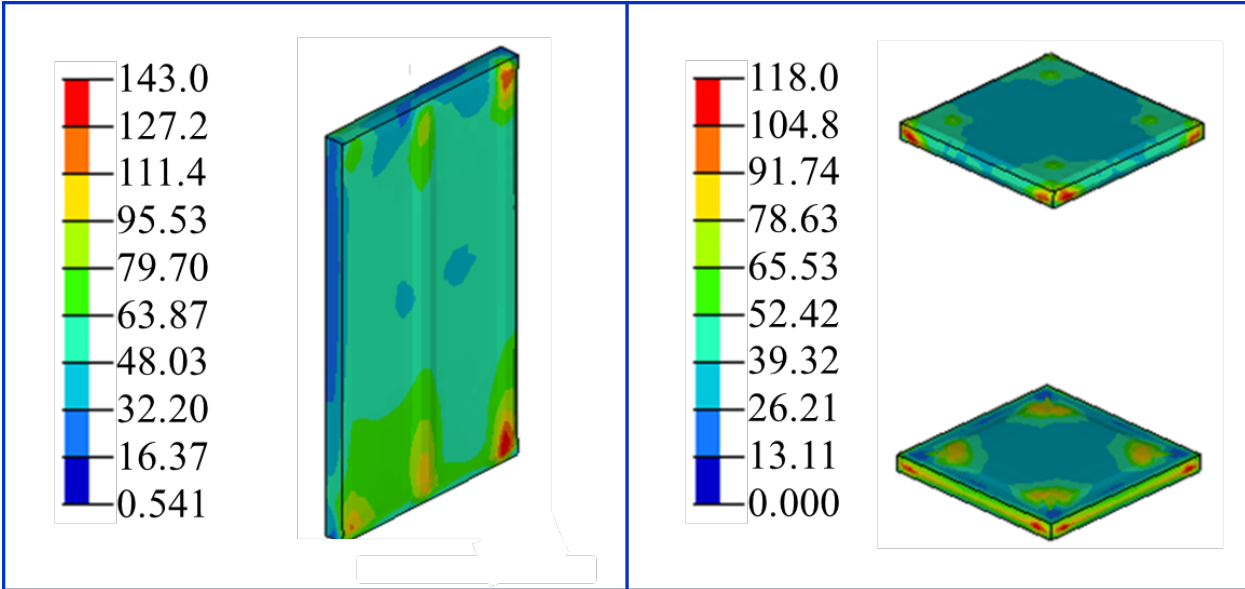


Figure 43. Displacements (Inch), Rectangular PCQS Concept (with Embedded Air Beams) at 15.0 psig



(a) Three Sidewalls with Embedded Air Beams

(b) Air Beams



(c) Rightmost Sidewall from (a)

(d) Roof and Floor Sections

Figure 44. Stresses (psi) of Rectangular PCQS Concept (with Embedded Air Beams) at 10.0 psig

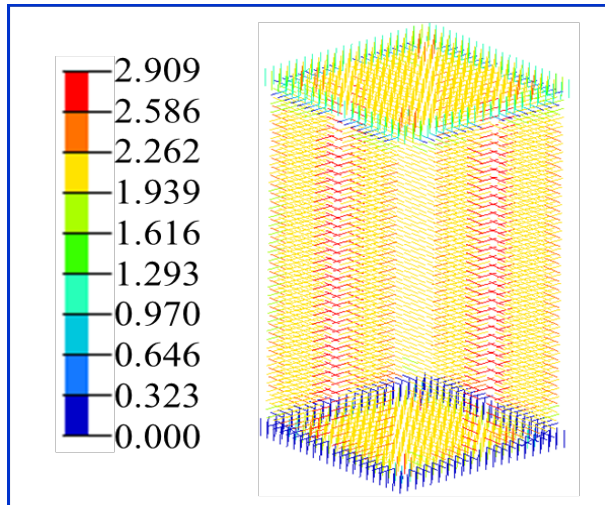


Figure 45. Drop-Yarn Tension Force (lbf) of PCQS Concept (with Embedded Air Beams) at 15.0 psig

The maximum volumes for each inflatable component as a function of inflation pressure are listed in table 4 and plotted in figure 46.

Table 4. Component Air Volumes of the Rectangular PCQS Concept with Embedded Air Beams

Inflation Pressure (psig)	Max Sidewall Volume (in. ³)	Max Floor Volume (in. ³)	Max Roof Volume (in. ³)	Max Corner Air Beam Volume (in. ³)	Max Mid-Span Air Beam Volume (in. ³)
5.0	13,660	8,885	8,935	1,230	878
10.0	14,025	8,990	9,150	1,232	874
15.0	14,710	9,200	9,470	1,245	880

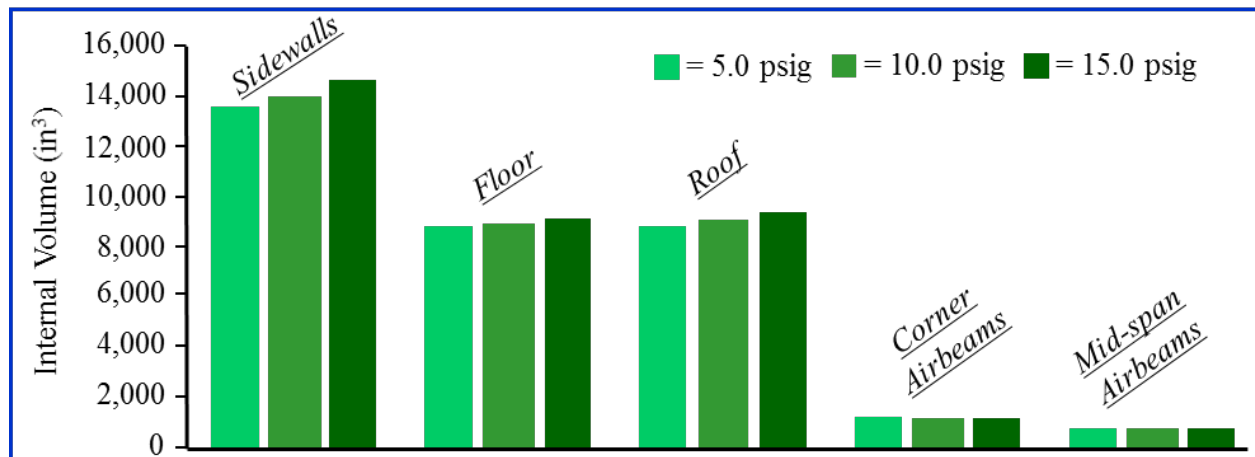


Figure 46. Air Volumes, Rectangular PCQS Concept (with Embedded Air Beams) Versus Pressure

The results listed in table 5 demonstrate in general that the skin tension forces per unit length increased with increasing inflation pressure. Notable exceptions to this, however, were the floor and roof panels (see figure 47). At 15.0-psig inflation pressure, the skin tensions decreased from the values produced by the 10.0-psig inflation case as a result of the continued constraining effects caused by the interacting air beams and sidewall panels. These effects resulted in a nonlinear behavior of the assembled PCQS.

Table 5. Skin Tension Force per Unit Length Results of the Rectangular PCQS Concept with Embedded Air Beams

Inflation Pressure (psig)	Max Sidewall Skin Tension (lbf/in.)	Max Floor Skin Tension (lbf/in.)	Max Roof Skin Tension (lbf/in.)	Max Air Beam Skin Tension (lbf/in.)
5.0	61.7	76.7	86.3	238.9
10.0	96.0	113.6	127.8	364.4
15.0	143.0	104.8	118.0	427.0

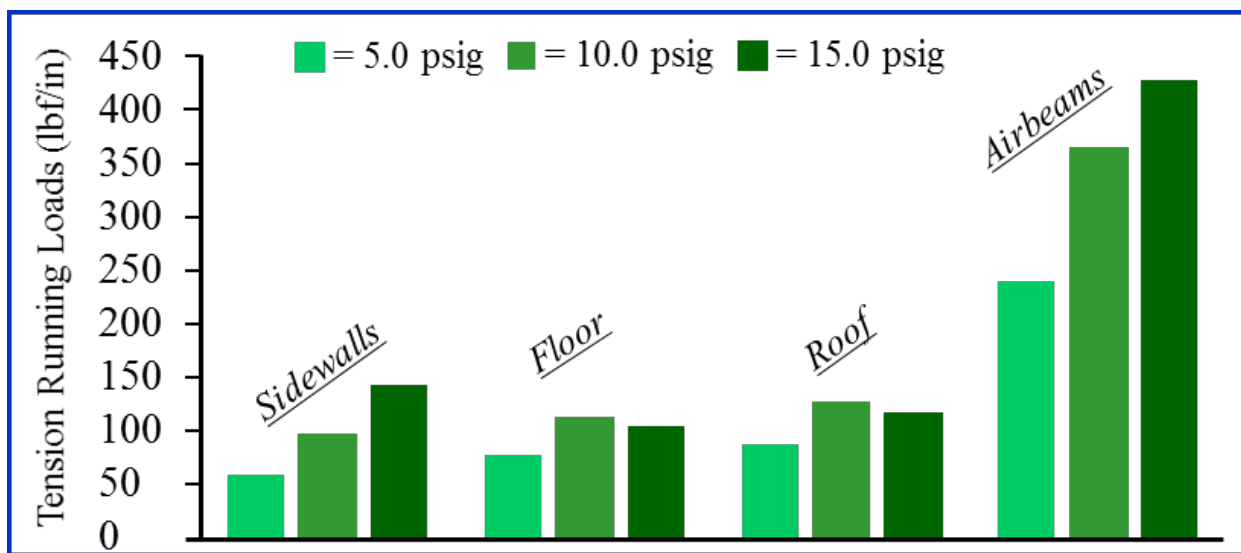


Figure 47. Peak Tension Running Loads (lbf/in.), Rectangular PCQS (with Embedded Air Beams)

A comparison of figures 31 and 46 demonstrates that structural coupling effects were more prevalent in the rectangular PCQS concept with embedded air beams versus the rectangular PCQS with the membrane line concept. The air beam skin tensions shown in figure 43 were nonlinear with increasing inflation pressure. The floor and roof skin tensions also shown in figure 43 did not increase monotonically with increasing inflation pressure as was observed in figure 31. The rectangular PCQS concept with embedded air beams, therefore, exhibited a higher level of geometric nonlinearities because of structural coupling of its components.

SUMMARY AND CONCLUSIONS

This preliminary study was undertaken to investigate the use of today's inflatable structures technologies to support conceptual development of protective crew quarters for use aboard manned spacecraft. Protection is sought to prevent exposure of the crew to harmful radiation levels resulting from both SPEs and GCRs.

The objectives were to develop simple water-filled structural concepts that would be easy to assemble/disassemble on-station for single-occupant use. The use of drop-stitch fabric panels and optional air-beam technologies would allow the redundant use of these panels and beams to serve as water storage bags, which are currently used on manned spacecraft.

Three concepts comprising drop-stitch fabrics and air beams were evaluated using finite element models: (1) a circular enclosure, (2) a rectangular enclosure with air beams and inner cushioning support, and (3) a rectangular concept with air beams embedded within the drop-stitch fabric panels. The air beams used in the rectangular concepts provided a skeletal framework for assembling the flat, drop-stitch fabric panels.

Finite element models of each concept were developed. The property used for the pressurization media for these models was air rather than water. Air was used to provide opportunities for direct correlation of the models with future planned experimental tests in which prototypes would be evaluated on land by using air to minimize the effects of gravity. Nominal 5.0-, 10.0-, and 15-psig inflation pressures were used for each model. Results included panel deflections, skin tensions, volume-versus-time histories, and drop-yarn tension forces. Although the analyses also included higher pressure cases of 10 psig and 15 psig, the 5.0-psig case is representative of actual usage; the higher pressure cases require further investigation via correlation with experimentation.

The circular PCQS was unable to develop the proper distribution of biaxial tensile stresses in the inner drop-stitch fabric skin, resulting in an unacceptable developed shape. The two rectangular PCQS concepts provided acceptable deployable shapes and were considered strong candidates for prototype fabrication and experimental evaluation. The rectangular PCQS concept with the IML was expected to require stowage volume greater than that of the rectangular PCQS concept with embedded air beams. Quantification of the deployed and stowed volume dimensions would be determined through actual physical testing.

REFERENCES

1. P. S. Bulson, "Design Principles of Pneumatic Structures," *The Structural Engineer*, vol. 51, no. 6, June 1973.
2. M. Stein, J. M. Hedgepeth, "Analysis of Partly Wrinkled Membranes," NASA Technical Note D-813, NASA Langley Research Center, Hampton, VA, July 1961.
3. W. Fichter, "A Theory for Inflated Thin-Wall Cylindrical Beams," NASA Technical Note D-3466, National Aeronautics and Space Administration, Washington, DC, 1966.
4. E. C. Steeves, "Behavior of Pressure Stabilized Beams Under Load," Technical Report 75-082-AMEL, United States Army Natick Development Center, Natick, MA, 1975.
5. P. Cavallaro and A. Sadegh, "Air-Inflated Fabric Structures," in *Mark's Standard Handbook for Mechanical Engineers, 11th Edition*, E. Avallone, T. Baumeister, and A. Sadegh, eds., McGraw-Hill, NY, 2006, pp. 20.108–20.118.
6. P. Cavallaro, M. Johnson, and A. Sadegh, "Mechanics of Plain-Woven Fabrics for Inflated Structures," *Composite Structures Journal*, vol. 61, 2003, pp. 375–393.
7. P. Cavallaro, A. Sadegh, and C. Quigley, "Decrimping Behavior of Uncoated Plain-Woven Fabrics Subjected to Combined Biaxial Tension and Shear Stresses," *Textile Research Journal*, vol. 77, no. 6, 2007, pp. 403–416.
8. P. Cavallaro, A. Sadegh, and C. Quigley, "Contributions of Strain Energy and PV-Work on the Bending Behavior of Uncoated Plain-Woven Fabric Air Beams," *Journal of Engineered Fibers and Fabrics*, vol. 2, no. 1, 2007, pp. 16–30.
9. J. Falls and J. Waters, "Bending Tests of Inflatable Dropstitch Panels," *11th International Conference on Fast Sea Transportation*, Honolulu, HI, September 2011.
10. J. Waters and J. Falls, "Bending Tests of Inflatable Dropstitch Panels," (draft), U.S. Naval Academy, Annapolis, MD, 2010.
11. S. Farboodmanesh, J. Chen, J. L. Mead, and K. White, "Effect of Construction on Mechanical Behavior of Fabric Reinforced Rubber," *Rubber Division Meeting, American Chemical Society*, Pittsburgh, PA, 8 – 11 October 2002.
12. P. Cavallaro, C. Quigley, and A. Sadegh, "Biaxial and Shear Testing Apparatus with Proportional Force Controls," U.S. Patent 7,204,160, 17 April 2007.

REFERENCES (Cont'd)

13. P. Cavallaro, C. Hart, A. Sadegh, "Mechanics of Air-Inflated Drop-Stitch Fabric Panels Subject to Bending Loads," *2013 ASME International Mechanical Engineering Congress and Exposition*, San Diego, CA, November 15–21, 2013.
14. Abaqus/Explicit, Ver. 6.10, Dassault Systèmes Waltham, MA.
15. "Structural Design and Test Factors of Safety for Spaceflight Hardware," NASA Technical Standard NASA-STD-5001B, National Aeronautics and Space Administration, Washington, DC, 6 August 2014.
16. T. C. Slaba, C. J. Mertens, S. R. Blattnig, "Radiation Shielding Optimization on Mars," NASA/TP–2013-217983, NASA Langley Research Center, Hampton, VA, 2013.
17. K. Wark, *Thermodynamics*, McGraw-Hill Book Co, 3rd edition, 1977.
18. "National Aeronautics and Space Administration," <http://msis.jsc.nasa.gov/images/Section03/Image64.gif>
19. "MsC-Technology-Anthropometrics," http://msc.-technology.wikispace.com/anthropometrics_4.gif/32338099/anthropometrics_4.gif

INITIAL DISTRIBUTION LIST

Addressee	No. of Copies
NASA Langley Research Center, Hampton, VA (R. Smith)	20
U.S. Army Natick Soldier Research, Development, and Engineering Center, Natick, MA (M. Jee, C. Quigley, K. Horak, J. Ward, G. Proulx, S. Tucker, P. Blanas, R. Benney, G. Thibault)	9
Navy Clothing and Textile Research Facility, Natick, MA (B. Avellini, A. Brayshaw, L. Caulfield, T. Hart, C. Heath)	5
Naval Surface Warfare Center, Panama City, FL (Code CX05 (F. Garcia))	1
Defense Technical Information Center	1
Center for Naval Analyses	1
City College of the City University of New York, NY (A. Sadegh)	1

